



Faculty of Science and Technology

MASTER'S THESIS

Study program/Specialization: Petroleum Geosciences Engineering	Spring semester, 2016 Open
Writer: Yichen Yang	(Writer's signature)
Faculty supervisor: Reidar B. Bratvold	
External supervisor(s):	
Title of thesis: A Reduced Order Model for Fast Production Prediction from an Oil Reservoir with a Gas Cap	
Credits (ECTS): 30	
Keywords: Production prediction Gas cap field Material balance equation Uncertainty assessment Monte Carlo simulation	Pages: 82 +enclosure: CD Stavanger, June 15 th 2016

Copyright

by

Yichen Yang

2016

**A Reduced Order Model for Fast Production Prediction from an Oil
Reservoir with a Gas Cap**

by

Yichen Yang, B.Sc.

Thesis

Presented to the Faculty of Science and Technology

The University of Stavanger

The University of Stavanger

June 2016

Acknowledgements

I would like to first express my sincere gratitude to my thesis supervisor Prof. Reidar B. Bratvold for his kind help and suggestions throughout the process of researching and writing this thesis. This accomplishment would not have been possible without you.

Besides my supervisor, I would like to particularly thank Philip Thomas, Aojie Hong, Kanokwan Kullawan and Camilo Malagon for their insightful comments and encouragement during my research.

Finally, I must express my very profound gratitude to my parents for providing me with consistent support and encouragement throughout my years of study.

Abstract

A Reduced Order Model for Fast Production Prediction from an Oil Reservoir with a Gas Cap

Yichen Yang, M.Sc.

The University of Stavanger, 2016

Supervisor: Reidar B. Bratvold

Economic evaluations are essential inputs for oil and gas field development decisions. These evaluations are critically dependent on the unbiased assessment of uncertainty in the future oil and gas production from wells. However, many production prediction techniques come at significant computational costs as they often require a very large number of highly detailed grid based reservoir simulations.

In this study, we present an alternative compelling and efficient approach to assess the impact of reserves uncertainty on the oil and gas production from an oil reservoir with a gas cap. The justification for using the reduced order (less detailed) model to assess possible future production is that, for many decisions, it is more important to capture the uncertainties in the production than the production impact of the detailed characteristics of the reservoir in question. The computational costs of the reduced order model presented in this work is small relative to a typical grid based simulator which makes it possible to assess production uncertainties by using Monte Carlo simulation with a large number of iterations.

The model developed in this work combines the use of inflow performance relationship (IPR), tubing performance relationship (TPR) curves with the material balance equation. By balancing the dynamic material balance equation at each time period, the reservoir average pressure decline curve and the oil and gas production profiles can be obtained. The impact of

reserves uncertainty on oil and gas production can be assessed by combining this approach with the Monte Carlo simulation method.

We apply the approach to a gas cap field to investigate the impact of reserves uncertainty on oil and gas production. The result shows that the relationship between oil in place, gas cap-to-oil volume ratio and oil production can be expressed in a functional form. One conclusion from this study is that the oil in place uncertainty has a larger impact on oil production than the gas in place uncertainty.

The approach in this study is developed in MATLAB and easy to modify and extend, so it can be applied to other gas cap fields and combined with cash flow model to help the decision maker design specific development and production plans and maximize the overall value of the field.

Table of Contents

Acknowledgements	iv
Abstract.....	v
Table of Contents	vii
List of Tables	viii
List of Figures.....	ix
Nomenclature	xi
1. Introduction.....	1
2. PVT Properties Analysis	4
3. Well Production Model.....	10
3.1 Inflow Performance Relationship (IPR)	10
3.2 Future IPR Prediction	12
3.3 Tubing Performance Relationship (TPR)	13
3.4 Natural Flow	24
3.5 Application of Material Balance Equation	26
3.6 Model Test and Verification	27
4. Uncertainty Analysis.....	36
4.1 Reserves Uncertainty	36
4.2 Monte Carlo Simulation.....	37
4.3 A Case Study.....	39
5. Discussion and Conclusion.....	51
References	53
Appendices.....	55

List of Tables

Table 1 Basic input parameters for model test.....	28
Table 2 Distribution of initial hydrocarbon in place in X gas cap field	39
Table 3 Basic input parameters in the X gas cap field.....	40

List of Figures

Figure 1 A typical gas cap drive reservoir (Dake, 1983).....	1
Figure 2 The typical production history of a gas cap drive reservoir (Solley and Sonnenberg, 2014)	1
Figure 3 The linear IPR curve (Golan and Whitson, 1991).....	10
Figure 4 The IPR curve for the saturated oil and gas wells (Golan and Whitson, 1991)	
.....	11
Figure 5 An example of current and future IPR curves	13
Figure 6 Computer flow diagram for the Beggs and Brill method	16
Figure 7 Horizontal flow pattern map.....	20
Figure 8 An example of typical TPR curve	23
Figure 9 Natural flow rate condition (Golan and Whitson, 1991)	24
Figure 10 Influence of wellhead pressure on natural flow rate	25
Figure 11 Influence of gas liquid ratio on natural flow rate	25
Figure 12 Influence of tubing inner diameter on natural flow rate.....	26
Figure 13 The general form of material balance equation.....	26
Figure 14 Solution gas oil ratio comparison	28
Figure 15 Oil formation volume factor comparison	29
Figure 16 Gas formation volume factor comparison	29
Figure 17 Gas viscosity comparison	30
Figure 18 Oil viscosity comparison	30
Figure 19 IPR curve comparison	31
Figure 20 TPR curve comparison	31
Figure 21 Oil production profile comparison (without gas reinjection)	32
Figure 22 Gas production profile comparison (without gas reinjection).....	32
Figure 23 Reservoir pressure declination comparison (without gas reinjection) ..	33
Figure 24 Oil production profile comparison (with gas reinjection)	33
Figure 25 Gas production profile comparison (with gas reinjection)	34

Figure 26 Reservoir pressure declination comparison (with gas reinjection).....	34
Figure 27 Three PERT distributions with different input parameters	37
Figure 28 The general procedures of Monte Carlo simulation (Bratvold and Begg, 2010)	38
Figure 29 The procedures of Monte Carlo simulation in this study	38
Figure 30 The probability distribution of oil in place.....	40
Figure 31 The probability distribution of gas cap-to-oil volume ratio	40
Figure 32 Running average of samples from oil in place distribution.....	41
Figure 33 Running standard deviation of samples from oil in place distribution..	42
Figure 34 The number of iterations and its corresponding computational time	42
Figure 35 Oil production profiles generated from 1000 iterations and its mean production profile	43
Figure 36 The relationship between oil and gas in place and oil production at four different years	43
Figure 37 The trend surface analysis for oil production at the 30 th year	44
Figure 38 The trend surface analysis for oil production at the 50 th year	44
Figure 39 The trend surface analysis for oil production at the 70 th year	45
Figure 40 The trend surface analysis for oil production at the 90 th year	45
Figure 41 The shifted and original distributions of oil in place.....	47
Figure 42 The shifted and original distributions of gas cap-to-oil volume ratio ...	47
Figure 43 The tornado chart to identify the main uncertainty driver.....	48
Figure 44 The relationship between oil in place and recovery efficiency	49
Figure 45 The relationship between gas cap-to-oil volume ratio and recovery efficiency	50

Nomenclature

English		
A	area	M_g gas molecular weight
B_g	gas formation volume factor	n total number of moles
B_o	oil formation volume factor	n flow exponent
B_w	water formation volume factor	NTG net-to-gross thickness ratio
$B(\theta)$	liquid holdup inclination	N stock tank oil initially in place
	correction factor	N_{FR} Froude number
c	isothermal compressibility	N_{Lv} liquid velocity number
c_f	pore compressibility	N_p cumulative oil production
C	flow coefficient	N_{Re} Reynolds number
D	tubing diameter	p pressure
e	exponential	p_{av} average pressure
f	friction factor	P_{pc} pseudocritical pressure
f_M	Moody friction factor	P_r pseudoreduced pressure
f_{tp}	two-phase friction	P_R reservoir pressure
f_n	no-slip friction factor	Δp pressure drop
f_w	water cut	q production rate
g	local acceleration due to gravity	R gas constant
g_c	gravitational constant	R_p production gas oil ratio
G	weight flux rate	R_s solution gas oil ratio
h	oil zone thickness	S saturation
$H_L(0)$	horizontal liquid holdup	S_{wc} connate water saturation
$H_L(\theta)$	liquid holdup	T absolute temperature
J	productivity index	T_{av} average temperature
L	length	T_{pc} pseudocritical temperature
ΔL	length increment	T_r pseudoreduced temperature
m	ratio of the initial hydrocarbon pore volume of the gas cap to that of the oil	T_R reservoir temperature
		v velocity
		V volume
		W_e cumulative natural water influx

W_p	cumulative natural water production	el	elevation
Z	z-factor	f	friction
Greek		g	gas
β	liquid holdup inclination correction factor coefficient	i	initial
γ	specific gravity	L	liquid
ε	absolute pipe roughness	n	no-slip
λ	no-slip liquid holdup	o	oil
θ	pipe inclination angle	od	dead oil
μ	viscosity	os	saturated oil
ρ	density	ou	undersaturated oil
σ	surface tension	p	production
ϕ	porosity	sc	standard condition
		SG	superficial gas
		SL	Superficial liquid
		t	mixture
acc	acceleration	tp	two-phase
av	average	w	water
b	bubble point	wh	wellhead
c	constant	wf	bottomhole flowing

1. Introduction

A gas cap field is an oil reservoir with a segregated free gas zone overlying an oil zone. In such reservoirs, the main producing mechanism is the expansion of the gas cap gas and solution gas, which pushes the oil downward to the production wells. For a typical gas cap field (Figure 1), the exploration well is drilled to identify the gas oil contact. Then all production wells are placed further down-dip since the purpose is not to produce gas but rather to allow its expansion to push the oil towards the production wells.

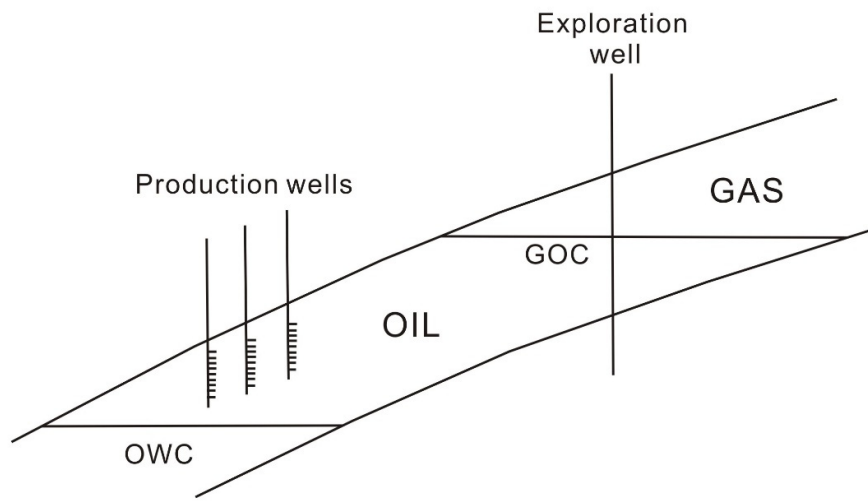


Figure 1 A typical gas cap drive reservoir (Dake, 1983)

It is known that reservoir pressure declines with production. Figure 2 shows the production history of a typical gas cap drive reservoir. The reservoir pressure and oil production drop steadily, while the gas oil ratio increases naturally.

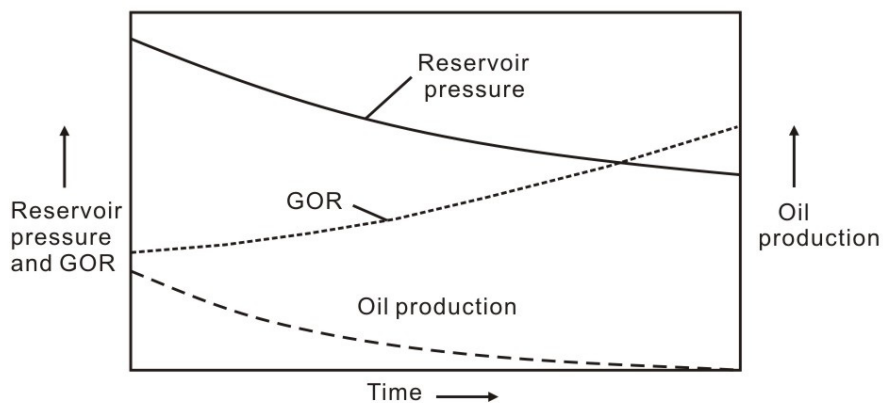


Figure 2 The typical production history of a gas cap drive reservoir (Selley and Sonnenberg, 2014)

One common method for improving the oil recovery in a gas cap field is to reinject a portion of the produced gas, if the economics are favorable. The reinjected gas helps maintaining the reservoir pressure. The theory behind this method is that gas reinjection will maximize the oil production and thus maximize the overall value of the reservoir. But in consideration of the uncertainty in future oil and gas prices, the method above may eventually not maximize the overall value of the reservoir (Thomas and Bratvold, 2015). In this case, an optimal time point can be identified when the gas should be lifted and sold rather than being reinjected. Switching from injecting to a depressurization of the gas cap reservoir is called gas cap blowdown.

The common way to identify the optimal blowdown time is to generate oil and gas production profiles for each possible blowdown time and compare the resulting values. The blowdown time with the highest value is optimal. However, many of the production prediction techniques come at significant computational costs, as they require a very large number of grid based reservoir simulations. This makes it difficult to identify the optimal blowdown time, not to mention to assess the impact of reserves uncertainty on oil and gas production.

The purpose of this thesis is to identify a compelling and efficient approach to assess the impact of reserves uncertainty on oil and gas production. Such an approach can be useful to identify production uncertainties for several different decision contexts including the blowdown decision with the goal of maximizing the overall value of the field. The specific objectives of this work are to:

- Develop a material balance based production model which can be used to generate cogent oil and gas production profiles at a relatively low computational expense
- Illustrate and assess the impact of reserves uncertainty on oil and gas production

In order to achieve these objectives, a six-step approach has been implemented:

- 1) Develop the production model by constructing inflow performance relationship (IPR) and tubing performance relationship (TPR)
- 2) Calculate the oil and gas production over a selected time period based on the production model
- 3) Select the appropriate oil PVT properties (e.g., B_o , B_g , R_s) to balance the material balance equation (MBE) based on the oil and gas reserves and production data
- 4) Identify the corresponding reservoir pressure based on the oil PVT properties used above
- 5) Generate the oil and gas production profiles by repeating steps 2 through 4 at each selected time period

- 6) Apply Monte Carlo simulation (MCS) to assess the impact of reserves uncertainty on oil and gas production

2. PVT Properties Analysis

The goal of pressure-volume-temperature (PVT) analysis is to determine the relationship between observed surface volumes of hydrocarbon production and the corresponding volume in the reservoir. A good knowledge of PVT properties will be helpful to the reserves calculation and its economic evaluation. Ideally, these properties are determined from laboratory studies on samples collected at an early stage in the reservoir's production life. There are usually two ways of collecting such samples, either by direct subsurface sampling or by surface recombination of oil and gas phases. However, such laboratory data are not always available because of cost saving and the strict measurement environment. In that situation, PVT properties can be approximated by using empirical correlations.

The three main PVT parameters measured from PVT analysis are solution gas oil ratio (R_s), oil formation volume factor (B_o) and gas formation volume factor (B_g), all of which are of primary importance in material balance calculation and well performance analysis.

The solution gas oil ratio (R_s) is the amount of surface gas that can be dissolved in one stock tank barrel of oil when both are at a specific reservoir pressure and temperature (units-scf/stb). The oil formation volume factor (B_o) is the ratio of the volume of oil at reservoir conditions to that at surface conditions (units-rb/stb). The gas formation volume factor (B_g) is the ratio of the volume of gas at reservoir conditions to that at surface conditions (units-rb/scf).

Many correlations have been developed in the petroleum industry to estimate the solution gas oil ratio (R_s), oil formation volume factor (B_o) and gas formation volume factor (B_g). Examples of such PVT correlations are given by Standing (1947), Lasater (1958), Glaso (1980), Al-Marhoun (1988), Petrosky and Farshad (1993). Each of these correlations seems to be applicable and reliable only for a specific set of reservoir fluid characteristics. This is due to the fact that each correlation has been developed by using samples from a restricted geographical area.

In this work, the Standing correlation is applied to calculate the solution gas oil ratio (R_s) and the oil formation volume factor (B_o). For a gas cap field, the oil is saturated and the reservoir pressure is equal to the bubble point pressure. Standing used 105 experimentally determined data points obtained from 22 different California crude oils to develop the correlations. In 1947, he published the equations to estimate the solution gas oil ratio (R_s) and the oil formation volume factor (B_o) when the reservoir pressure is equal to the bubble point pressure.

Solution gas oil ratio

$$R_s = \gamma_g \left((1.4 + p/18.2)^{1.205} 10^{(0.0125\gamma_{API}-0.00091T)} \right)^{1/0.83} \quad (1)$$

Oil formation volume factor

$$B_o = 0.972 + 1.47 \times 10^{-4} \times \left(1.25T + R_s(\gamma_g/\gamma_o)^{1/2} \right)^{1.175} \quad (2)$$

Standing used flash liberation tests to obtain the experimental data and he stated that, for the given data set, the average error in using equations (1) and (2) are 4.8% and 1.2%, respectively. The oil samples used during the experimental process were free of nitrogen (N_2) and hydrogen sulfide (H_2S), with CO_2 less than 1 mole percent. In this work, it is also assumed that the gas in the gas cap field doesn't contain the nitrogen (N_2), hydrogen sulfide (H_2S) and carbon dioxide (CO_2).

Gas formation volume factor

The gas formation volume factor (B_g) can be deduced by the simple equation of state

$$pV = ZnRT \quad (3)$$

in which Z is called the Z -factor and is the ratio of the real volume to the ideal volume, which defines the departure from the ideal gas behavior. R is the gas constant.

By applying equation (3) at both standard and reservoir conditions, the gas formation volume factor becomes

$$B_g = \frac{V_R}{V_{SC}} = \frac{p_{sc}}{p} \cdot \frac{T}{T_{sc}} \cdot \frac{Z}{Z_{sc}} \quad (4)$$

For the standard condition of $p_{sc} = 14.7$ pisa, $T_{sc} = (460 + 60) = 520^{\circ}R$ and $Z_{sc} = 1$, equation (4) can be reduced to

$$B_g = 0.00503676 \frac{ZT}{p} \quad (5)$$

Before equation (5) can be used for gas formation volume factor calculation, the Z -factor should be measured. Z -factors can be determined through several steps, starting with the estimation of the pseudocritical temperature T_{pc} and pseudocritical pressure P_{pc} of gas mixtures. Based on the definition, the pseudocritical temperature T_{pc} and pseudocritical pressure P_{pc} can normally be calculated by the mole average of critical temperature and

pressure of the mixture components. There are different correlations available for pseudocritical property estimation. One correlation is developed by Sutton (1985) based on 264 different gas samples, which is used in this work.

Pseudocritical temperature

$$T_{pc} = 169.2 + 349.5\gamma_g - 74.0\gamma_g^2 \quad (6)$$

Pseudocritical pressure

$$P_{pc} = 756.8 - 131.07\gamma_g - 3.6\gamma_g^2 \quad (7)$$

After the pseudocritical properties are obtained, the next step is to calculate the pseudoreduced temperature T_r and pressure P_r by using the following equations.

$$T_r = \frac{T}{T_{pc}} \text{ and } P_r = \frac{p}{P_{pc}} \quad (8)$$

Then the Z-factor can be determined by using the Standing-Katz correlation chart (1942), which has shown itself to be very reliable and is considered as the industry standard. Several best-fit equations for the Standing-Katz correlation chart have been developed, such as Hall and Yarborough (1973), Dranchuk and Abou-Kassem (1975) and Beggs and Brill (1973), which are more convenient for estimating the Z-factor in computer programs and spreadsheets. In this work, the Beggs and Brill equation is used for the Z-factor calculation.

Beggs and Brill correlation for Z-factor

$$Z = A + (1 - A)/e^B + CP_r^D \quad (9)$$

where

$$A = 1.39(T_r - 0.92)^{0.5} - 0.36T_r - 0.101 \quad (10)$$

$$B = (0.62 - 0.23T_r)P_r + \left[\frac{0.066}{(T_r - 0.86)} - 0.037 \right] P_r^2 + \frac{0.32}{10^{9(T_r-1)}} P_r^6 \quad (11)$$

$$C = (0.132 - 0.32 \log T_r) \quad (12)$$

$$D = 10^{(0.3106 - 0.49T_r + 0.1824T_r^2)} \quad (13)$$

Some useful correlations for other PVT parameters are introduced here to help to build the well production model in the following chapters.

Gas viscosity

For gas viscosity, Lee et al (1966) presented a useful empirical equation for most natural gas viscosity estimations, which is convenient for computer programming. The method uses the temperature, pressure, Z-factor, and molecular weight.

$$\mu_g = K_1 \exp(X \rho_g^Y) \quad (14)$$

where

$$\rho_g = 0.00149406 \frac{p M_g}{Z T} \quad (15)$$

$$K_1 = \frac{(0.00094 + 2 \times 10^{-6} M_g) T^{1.5}}{(209 + 19 M_g + T)} \quad (16)$$

$$X = 3.5 + \frac{986}{T} + 0.01 M_g \quad (17)$$

$$Y = 2.4 - 0.2X \quad (18)$$

$$M_g = 28.967 \gamma_g \quad (19)$$

μ_g is gas viscosity, cP. ρ_g is gas density, g/cm³. p is pressure, psia. T is temperature, R. M_g is gas molecular weight.

Saturated oil viscosity

Beggs and Robinson (1975) developed a correlation which can be used for both dead and saturated oil viscosity.

$$\mu_{os} = A(\mu_{od})^B \quad (20)$$

where

$$\mu_{od} = 10^x - 1.0 \quad (21)$$

$$x = T^{-1.163} \exp(6.9824 - 0.04658\gamma_{API}) \quad (22)$$

$$A = 10.715(R_s + 100)^{-0.515} \quad (23)$$

$$B = 5.440(R_s + 150)^{-0.338} \quad (24)$$

μ_{os} is saturated oil viscosity, cP. μ_{od} is dead oil viscosity, cP. T is temperature, F. γ_{API} is oil API gravity, API. R_s is solution gas oil ratio, scf/stb.

Undersaturated oil viscosity

Undersaturated oil viscosity can be calculated by applying Vazquez and Beggs (1980) correlation.

$$\mu_{ou} = \mu_{ob} \left(\frac{p}{p_b} \right)^m \quad (25)$$

where

$$m = C_1 p^{C_2} \exp(C_3 + C_4 p) \quad (26)$$

$$C_1 = 2.6, C_2 = 1.187, C_3 = -11.513 \text{ and } C_4 = -8.98 \times 10^{-5} \quad (27)$$

μ_{ou} is undersaturated oil viscosity at $p > p_b$, cP. μ_{ob} is saturated oil viscosity at p_b , cP. p is pressure, psia. p_b is bubble-point pressure, psia.

Water viscosity

Brill and Beggs (1973) developed one simple relationship between water viscosity and temperature

$$\mu_w = \exp(1.003 - 0.01479T + 1.982 \times 10^{-5}T^2) \quad (28)$$

Where T is temperature, F.

Oil-gas interfacial tension

Abdul-Majeed and Al-Soof (2000) provided one equation to estimate the oil-gas surface tension

$$\sigma_o = (1.17013 - 1.694 \times 10^{-3}T)(38.085 - 0.259\gamma_{API}) \quad (29)$$

Where T is temperature, F. γ_{API} is oil API gravity, API.

Water-oil interfacial tension

Water-oil interfacial tension can be calculated using the following correlation proposed by Hough et al. (1951)

$$\sigma_{74} = 75 - 1.108p^{0.349}, T \leq 74^{\circ}\text{F} \quad (30)$$

$$\sigma_{280} = 53 - 0.1048p^{0.637}, T \geq 280^{\circ}\text{F} \quad (31)$$

$$\sigma_T = \sigma_{74} - \frac{(T - 74)(\sigma_{74} - \sigma_{280})}{206}, 74^{\circ}\text{F} \leq T \leq 280^{\circ}\text{F} \quad (32)$$

Where T is temperature, F . p is pressure, psia.

There are constraints and limitations in all of these empirical equations, but the results obtained by using these correlations are useful to estimate the impact of reserves uncertainty on oil and gas production. By using the correlations presented above, the PVT parameters can be estimated, which can be applied to build the well production model and material balance calculation in next steps.

3. Well Production Model

This chapter discusses a common method to build one well production model by using the inflow performance relationship (IPR) and tubing performance relationship (TPR). The model provides the relationship between the pressure and the flow rate and, will be used to predict the production rate.

3.1 Inflow Performance Relationship (IPR)

The inflow performance relationship (IPR) is the relationship between the surface flow rate q and the bottomhole flowing pressure P_{wf} at a given reservoir pressure P_R . It describes that the flow rate of fluids from the reservoir into the well is a function of the bottomhole flowing pressure (Guo et al., 2011). For an oil production well, the IPR equation is linear when the oil is undersaturated or slightly compressible (Golan and Whitson, 1991). It means that the fluid inflow rate is proportional to the difference between reservoir pressure and the bottomhole flowing pressure (Figure 3). When the bottomhole flowing pressure is equal to zero, the flow rate is the maximum rate $q_{o,max}$ which is called absolute open flow (AOF).

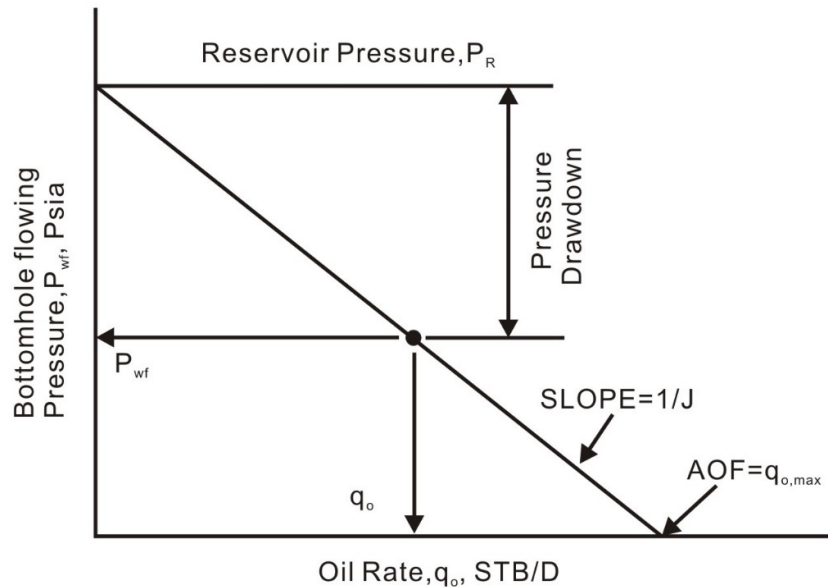


Figure 3 The linear IPR curve (Golan and Whitson, 1991)

The linear IPR can be represented by the following equation (Golan and Whitson, 1991)

$$q_o = J(P_R - P_{wf}) \quad (33)$$

where J is the productivity index (units – STB/D/psi), defined as the ratio of the flow rate to pressure drop in the reservoir. P_R is the average reservoir pressure.

For saturated oil and gas wells, the linear IPR is not suitable due to the effect of highly compressible gas and two-phase flow on IPR. Instead of a linear flow rate increase with pressure drop, it has been observed that larger-than-linear pressure drops are required to increase the rate at higher rates (Golan and Whitson, 1991). The IPR shows the curvature pronounced (Figure 4).

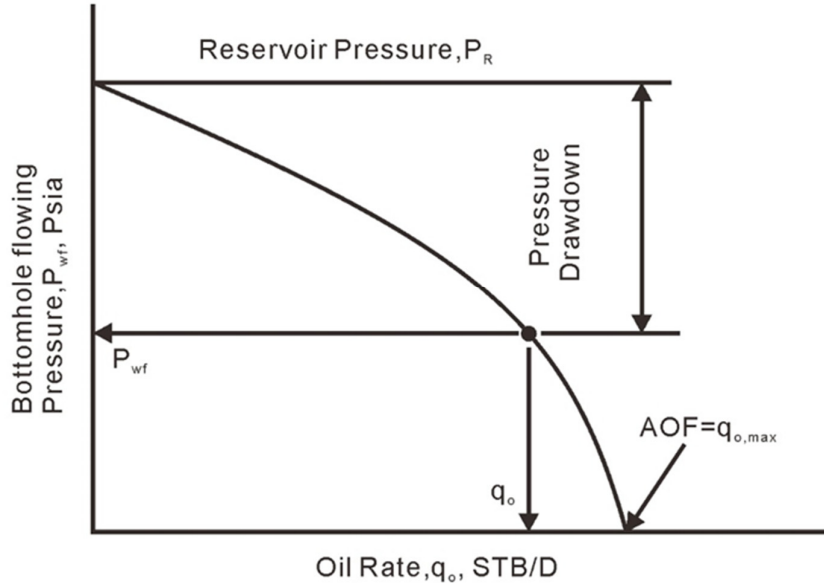


Figure 4 The IPR curve for the saturated oil and gas wells (Golan and Whitson, 1991)

Vogel (1968) proposed the following equation to describe the IPR curve for saturated oil wells:

$$\frac{q_o}{q_{o,max}} = 1 - 0.2 \left(\frac{P_{wf}}{P_R} \right) - 0.8 \left(\frac{P_{wf}}{P_R} \right)^2 \quad (34)$$

where $q_{o,max}$ is the maximum oil rate when bottomhole flowing pressure P_{wf} equals zero. Besides Vogel there are other correlations which describe two-phase inflow performance relationships, such as the equation presented by Fetkovich (1973). Vogel's equation is a best-fit approximation of numerous simulated well performance calculations. In this work, Vogel's equation is used to describe the IPR for saturated oil in gas cap reservoirs.

For gas well performance, the backpressure equation (Rawlins and Schellhardt, 1935) is widely accepted as a simple and accurate expression of the production:

$$q = C \left(P_R^2 - P_{wf}^2 \right)^n \quad (35)$$

where the exponent n ranges in value from 0.5 to 1.0 depending on flow characteristics and C is the flow coefficient.

The C and n can be determined by using a two or three point flow test and the following equation:

$$n = \frac{\log\left(\frac{q_1}{q_2}\right)}{\log\left(\frac{P_R^2 - P_{wf1}^2}{P_R^2 - P_{wf2}^2}\right)} \text{ and } C = \frac{q_1}{[P_R^2 - P_{wf1}^2]^n} \quad (36)$$

Where q_1 is the flow rate at bottomhole flowing pressure, P_{wf1} , and q_2 is the flow rate at bottomhole flowing pressure, P_{wf2} .

3.2 Future IPR Prediction

The future IPR prediction is key to forecast the future well production. Several methods exist to estimate the future maximum flow rate $q_{o,max}$. Usually these methods provide an equation relating changes in the productivity index J to the average reservoir pressure. Fetkovich (1973) presented the following equations to predict the maximum future flow rate:

$$q = J(P_R^2 - P_{wf}^2)^n \text{ and } J_2 = J_1(P_{R2}/P_{R1}) \quad (37)$$

where the flow exponent, n, is assumed to be constant throughout the entire production life of the reservoir. J_1 is the flow constant at current reservoir pressure, P_{R1} , and J_2 is the flow constant at a future reservoir pressure, P_{R2} .

When n and J_1 are determined by a few flow test points, then any future maximum flow rate $q_{o,max}$ can be estimated by

$$q_{o,max} = J_2(P_{R2}^2)^n \quad (38)$$

Based on Fetkovich's work, Eickmeier (1968) proposed a simple equation to estimate the maximum flow rate $q_{o,max}$. Instead of using multipoint test data, only one single flow test point is need to estimate the maximum flow rate $q_{o,max}$. Eickmeier (1968) set the flow exponent to a fixed value of 1 to arrive at

$$q_{o,max2} = q_{o,max1}(P_{R2}/P_{R1})^3 \quad (39)$$

After this relationship between the maximum flow rate and the reservoir pressure is established, for any future pressure, the corresponding maximum flow rate can be predicted. Then both values can be used in Vogel's IPR equation to generate a set of future IPR curves (Figure 5).

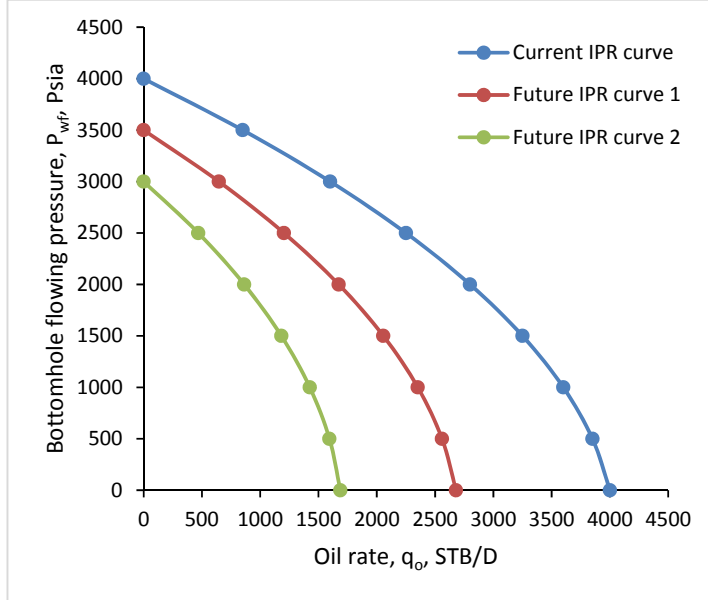


Figure 5 An example of current and future IPR curves

3.3 Tubing Performance Relationship (TPR)

A pressure difference between the bottomhole flowing pressure P_{wf} and the wellhead pressure P_{wh} is required to lift a fluid through the production tubing at a given surface flow rate q . For a specific wellhead pressure, the relationship between the bottomhole flowing pressure P_{wf} and the surface flow rate q is called tubing performance relationship (TPR). In order to generate the TPR curve, the pressure drop along the production tubing needs to be calculated at a given flow rate. Then the bottomhole flowing pressure can be determined by combining the specific wellhead pressure and the total pressure drop.

For single-phase conditions, like gas or highly undersaturated oil, the pressure drop can be calculated by conventional pipe flow equations. A convenient and accurate equation to display the TPR curve for a single-phase gas flow was presented by Katz et al (1959) using average temperature and Z-factor.

$$q_g = 200000 \left[\frac{sD^5(P_{wf}^2 - e^s P_{wh}^2)}{\gamma_g T Z H f_M (e^s - 1)} \right]^{0.5} \quad (40)$$

Where q_g is gas flow rate, scf/D. Z is average Z-factor. T is the average temperature, R. γ_g is gas gravity, air = 1. D is tubing diameter, in. P_{wf} is the bottomhole flowing pressure, psia. P_{wh} is the wellhead pressure, psia. H is the vertical depth, ft. $s = 0.0375 \gamma_g H / TZ$. f_M is the Moody friction factor.

A best-fit equation to estimate f_M for gas wells is the following expression, which is sufficiently accurate for most engineering calculations.

$$f_M = \{2 \log[3.71/(\varepsilon/D)]\}^{-2} \quad (41)$$

Where ε is the absolute pipe roughness for most commercial pipes and equal to 0.0006 in. For multiphase conditions, the tubing performance relationship is more complicated. This is due to the fact that the properties of each fluid and the interactions between each phase must be taken into account. The TPR curve can only be described approximately by the empirical equations. The theoretical basis for the pressure drop calculation is the mechanical balance equation. It is an expression for the balance of energy between two points in a system, which is composed of three distinct components.

The general differential form can be written as

$$\frac{dp}{dL} = \left(\frac{\partial p}{\partial L}\right)_{el} + \left(\frac{\partial p}{\partial L}\right)_f + \left(\frac{\partial p}{\partial L}\right)_{acc} \quad (42)$$

Where $\left(\frac{\partial p}{\partial L}\right)_{el}$ is the component due to hydrostatic pressure loss, $\left(\frac{\partial p}{\partial L}\right)_f$ is the component due to friction pressure loss, and $\left(\frac{\partial p}{\partial L}\right)_{acc}$ is the component due to kinetic pressure loss or convective acceleration.

For most applications, the kinetic pressure loss is very small and can be ignored. Thus, the equation that describes the overall pressure loss can be expressed as the sum of two terms:

$$\frac{dp}{dL} = \left(\frac{\partial p}{\partial L}\right)_{el} + \left(\frac{\partial p}{\partial L}\right)_f \quad (43)$$

The hydrostatic pressure loss calculation can be calculated by using a mixture density ρ_t :

$$\left(\frac{\partial p}{\partial L}\right)_{el} = \rho_t \frac{g \sin \theta}{g_c} \quad (44)$$

Where g is the local acceleration due to gravity, and g_c is the gravitational constant 32.174 ft/s². θ is the inclination angle of the pipe from horizontal.

Based on the definition, the friction pressure loss can be estimated by the following equation:

$$\left(\frac{\partial p}{\partial L}\right)_f = \frac{f_{tp} G_t v_t}{2 g_c D} \quad (45)$$

Where f_{tp} is the two-phase friction, G_t is the mixture weight flux rate, and v_t is the mixture velocity. D is the tubing diameter.

Some correlations have been presented to predict these pressure losses (Beggs and Brill, 1973; Duns and Ros, 1963; Hagedorn and Brown, 1965; Hasan and Kabir, 1992; Orkiszewski, 1967). In this study, the Beggs and Brill correlation is chosen to generate the TPR curve, based on the fact that it is relatively easily implemented in MATLAB or Excel VBA and perform as well as any of the other correlations. This method requires an iterative procedure for the two-phase pressure drop calculation. In the calculation, the pipe line is divided into a number of pressure increments, then the fluid properties and pressure gradient are evaluated at average pressure and temperature condition in each increment.

The procedure for segmenting the pipe line by pressure increment (Beggs and Brill, 1973) is:

Step 1: Starting with the known pressure, p_1 , at location L_1 , select a length increment ΔL , at least $\leq 10\%$ of total L .

Step 2: Estimate the incremental pressure change, Δp , corresponding to the length increment ΔL .

Step 3: Calculate the average pressure and temperature in the increment.

Step 4: Using empirical equations, determine the necessary PVT properties at average pressure and temperature in the increment.

Step 5: Calculate the pressure gradient, $\Delta p/\Delta L$, in the increment at average pressure and temperature condition.

Step 6: Determine the total incremental pressure change corresponding to the selected length increment, $\Delta p = \Delta L * (\Delta p/\Delta L)$.

Step 7: Compare the estimated and calculated values of Δp obtained in step 2 and 6. If they are not close enough, use the calculated incremental pressure and return to step 2. Repeat step 3 through step 7 until the estimated and calculated values are sufficiently close.

Step 8: Continue iteration until $L_1 + \sum \Delta L = L$ (total length), the bottomhole flowing pressure $p = p_1 + \sum \Delta p$.

Based on the procedure above, a computer flow diagram (Figure 6) is developed for calculating the two-phase pressure drop in a well.

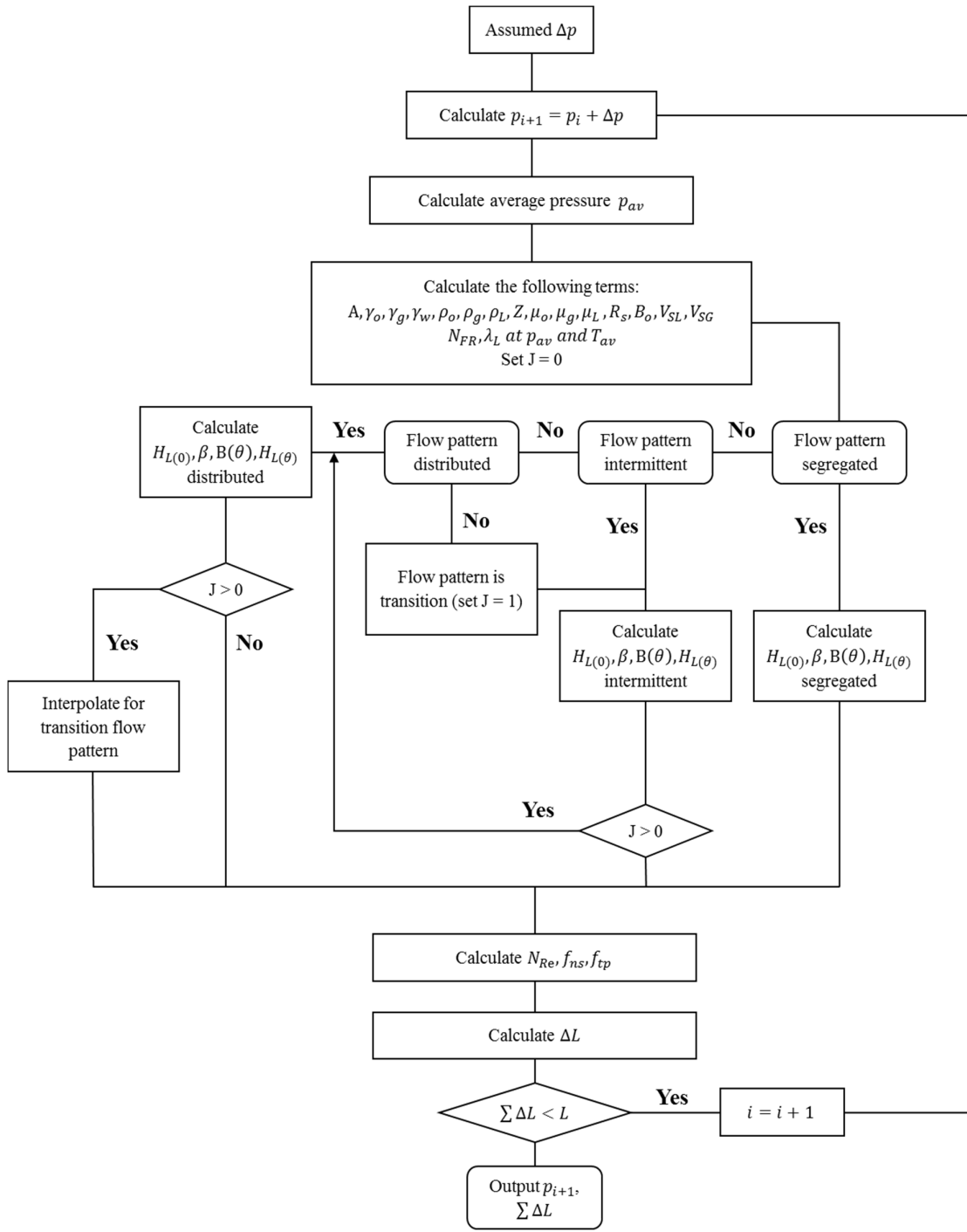


Figure 6 Computer flow diagram for the Beggs and Brill method

A detailed procedure for this two-phase pressure drop calculation is following:

1. Start with the known pressure, p_1 , at location L_1 , select a length increment ΔL , at least $\leq 10\%$ of total L .
2. Estimate the incremental pressure change, Δp , corresponding to the length increment ΔL .
3. Calculate the average pressure between the two points:

$$p_{av} = \frac{p_1 + (\Delta p + p_1)}{2}$$

4. Determine the average temperature T_{av} at the average depth, based on the temperature versus depth plot.
5. From PVT analysis or appropriate correlations, calculate solution gas oil ratio R_s , oil formation volume factor B_o , Z-factor and gas formation volume factor B_g .
6. Calculate gas, oil and water viscosity (μ_g, μ_o, μ_w), oil-gas interfacial tension σ_o and water-oil interfacial tension σ_w .
7. Calculate the oil gravity γ_o from API gravity:

$$\gamma_o = \frac{141.5}{131.5 + \gamma_{API}}$$

8. Calculate the gas ,oil and liquid densities at the average conditions of pressure and temperature:

$$\rho_g = \frac{28.97\gamma_g p_{av}}{ZRT_{av}}$$

$$\rho_o = \frac{350\gamma_o + 0.0764\gamma_g R_s}{5.615B_o}$$

$$f_w = \frac{q_w}{q_L} \text{ and } f_o = 1 - f_w$$

$$\rho_L = \rho_o(1 - f_w) + \rho_w f_w$$

9. Calculate the gas and liquid flowrate:

$$q_g = \frac{q_o(R_p - R_s)B_g}{86400}$$

$$q_L = \frac{[q_L(1 - f_w)B_o + q_L f_w B_w]5.615}{86400}$$

10. Calculate sectional area of pipe and the superficial gas, liquid and mixture velocity:

$$A = \pi(D/2)^2$$

$$v_{SG} = q_g/A$$

$$v_{SL} = q_L/A$$

$$v_t = v_{SG} + v_{SL}$$

11. Calculate the gas, liquid and mixture weight flux rates:

$$G_g = \rho_g v_{SG}$$

$$G_L = \rho_L v_{SL}$$

$$G_t = G_g + G_L$$

12. Calculate the no-slip liquid holdup:

$$\lambda = \frac{q_L}{q_g + q_L}$$

13. Calculate the Froude number:

$$N_{FR} = \frac{V_t^2}{gD}$$

14. Calculate liquid viscosity and mixture viscosity:

$$\mu_L = \mu_o(1 - f_w) + \mu_w f_w$$

$$\mu_t = \mu_g(1 - \lambda) + \mu_L \lambda$$

15. Calculate liquid interfacial tension:

$$\sigma_L = \sigma_o(1 - f_w) + \sigma_w f_w$$

16. Calculate the no-slip Reynolds number and the liquid velocity number:

$$N_{Re} = \frac{G_t D}{\mu_t}$$

$$N_{Lv} = 1.938 v_{SL} \left(\frac{q_L}{\sigma_L} \right)^{0.25}$$

17. Calculate the variables which will be used to determine the flow pattern if when the flow are horizontal:

$$L_1 = 316 \lambda^{0.302}$$

$$L_2 = 0.0009252 \lambda^{-2.4684}$$

$$L_3 = 0.10 \lambda^{-1.4516}$$

$$L_4 = 0.5 \lambda^{-6.738}$$

18. Determine the horizontal flow pattern (Figure 7) by using the following limits:

Segregated

$$\lambda < 0.01 \text{ and } N_{FR} < L_1$$

or

$$\lambda \geq 0.01 \text{ and } N_{FR} < L_2$$

Transition

$$\lambda \geq 0.01 \text{ and } L_2 \leq N_{FR} \leq L_3$$

Intermittent

$$0.01 \leq \lambda < 0.4 \text{ and } L_3 < N_{FR} \leq L_1$$

or

$$\lambda \geq 0.4 \text{ and } L_3 < N_{FR} \leq L_4$$

Distributed

$$\lambda < 0.4 \text{ and } N_{FR} \geq L_1$$

or

$$\lambda \geq 0.4 \text{ and } N_{FR} > L_4$$

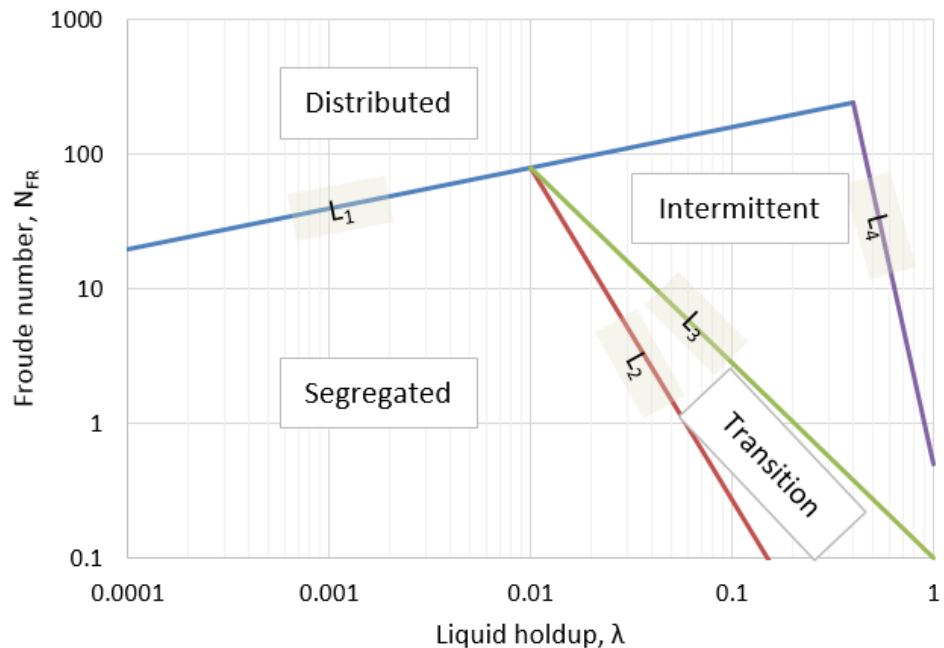


Figure 7 Horizontal flow pattern map

19. Calculate the horizontal liquid holdup:

$$H_L(0) = \frac{a\lambda^b}{N_{FR}^c}$$

where a, b and c are determined for different flow pattern from the following table:

Flow pattern	a	b	c
Segregated	0.98	0.4846	0.0868
Intermittent	0.845	0.5351	0.0173
Distributed	1.065	0.5824	0.0609

20. Calculate the liquid holdup inclination correction factor coefficient:

$$\beta = (1 - \lambda) \ln(d \lambda^e N_{Lv}^f N_{FR}^g)$$

where d, e, f and g are determined for different flow pattern from the following table:

Flow pattern	d	e	f	g
Segregated	0.011	-3.768	3.539	-1.614
Intermittent	2.96	0.305	-0.4473	0.0978
Distributed	No correlation $\beta = 0$			

21. Calculate the liquid holdup inclination correction factor:

$$B(\theta) = 1 + \beta[\sin(1.8\theta) - (1/3) \sin^3(1.8\theta)]$$

For vertical well, $\theta = 90^\circ$ and $B(\theta)$ becomes:

$$B(\theta) = 1 + 0.3\beta$$

22. Calculate the liquid holdup:

$$H_L(\theta) = H_L(0) B(\theta)$$

When the flow pattern is transition, the transition horizontal holdup should be determined by using both segregated horizontal holdup and intermittent horizontal holdup with following equations:

$$H_L(\theta)_{transition} = A \times H_L(\theta)_{Segregated} + B \times H_L(\theta)_{Intermittent}$$

where

$$A = \frac{L_3 - N_{FR}}{L_3 - L_2}$$

$$B = 1 - A$$

23. Calculate the two-phase density:

$$\rho_t = \rho_L H_L(\theta) + \rho_g (1 - H_L(\theta))$$

24. Calculate the pressure gradient due to the hydrostatic pressure loss:

$$\left(\frac{\partial p}{\partial L} \right)_{el} = \rho_t \frac{g \sin \theta}{g_c}$$

25. Calculate the ratio of two-phase to no-slip friction factor:

$$\frac{f_{tp}}{f_n} = e^S$$

where

$$S = [\ln(y)] / \{-0.0523 + 3.182 \ln(y) - 0.8725[\ln(y)]^2 + 0.01853[\ln(y)]^4\}$$

and

$$y = \frac{\lambda}{[H_L(\theta)]^2}$$

If y is in the interval $1 < y < 1.2$, the value of S is calculated from:

$$S = \ln(2.2y - 1.2)$$

26. Calculate no-slip friction factor from Darcy-Weisbach friction factor f :

$$f_n = f/4$$

where f can be obtained from Colebrook White equation:

$$\frac{1}{\sqrt{f}} = -2 \log_{10} \left(\frac{\varepsilon}{3.7D} + \frac{2.51}{N_{Re} \sqrt{f}} \right)$$

The Colebrook White equation can be solved by iteration using the Newton-Raphson method.

27. Calculate the two-phase friction factor

$$f_{tp} = \frac{f_{tp}}{f_n} f_n$$

28. Calculate the pressure gradient due to the friction pressure loss

$$\left(\frac{\partial p}{\partial L}\right)_f = \frac{f_{tp} G_t V_t}{2 g_c D}$$

29. Calculate the overall pressure gradient:

$$\frac{dp}{dL} = \left(\frac{\partial p}{\partial L}\right)_{el} + \left(\frac{\partial p}{\partial L}\right)_f$$

30. Calculate the overall pressure loss in this length increment ΔL :

$$\Delta p = \frac{dp}{dL} \Delta L$$

By repeating the procedure above at different oil rates, a TPR curve can be generated. The figure below shows a typical TPR curve (Figure 8).

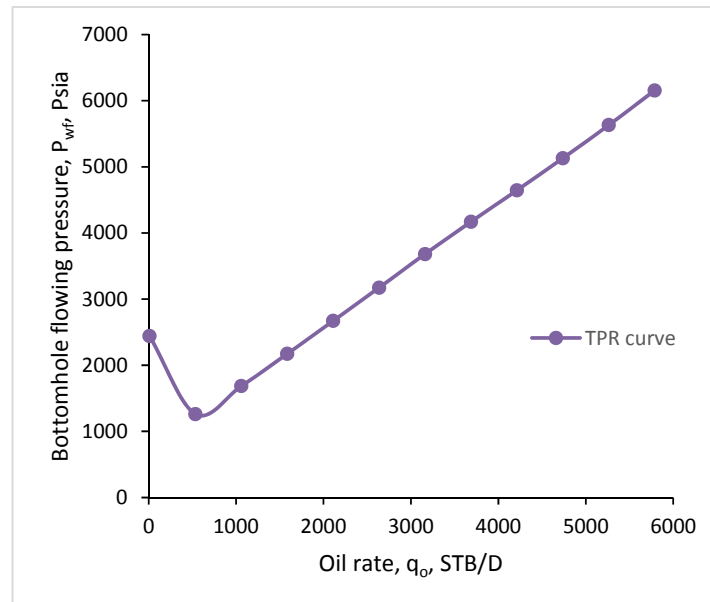


Figure 8 An example of typical TPR curve

3.4 Natural Flow

After the IPR curve and TPR curve are generated, the natural flow rate can easily be found. For a typical case, when at a specific rate the bottomhole flowing pressures of two curves are equal, the flow system is in equilibrium and the flow is stable (Golan and Whitson, 1991). This specific rate is called natural flow rate. Figure 9 illustrates the natural flow rate condition.

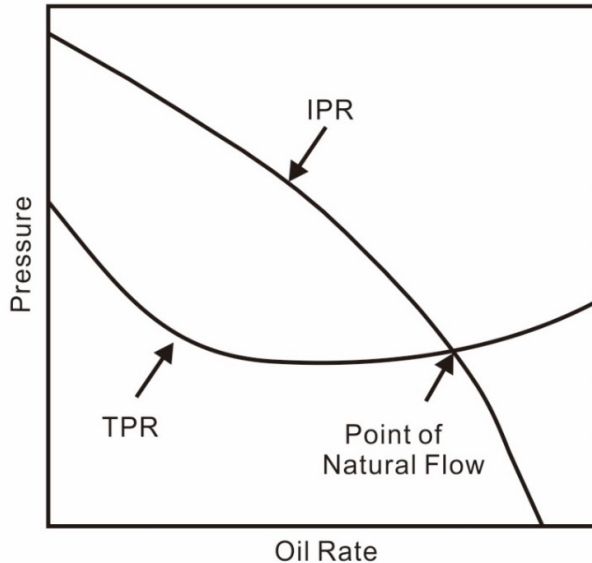


Figure 9 Natural flow rate condition (Golan and Whitson, 1991)

The natural flow rate will change with time, due to the changes of the IPR and TPR curves caused by the pressure change in reservoir. The other major factors influencing the natural flow rate are the well parameters, which have a great impact on the TPR curve based on the equations introduced in the previous section. The influence on the TPR curve of changing some of the main well parameters are described below.

Changing wellhead pressure

The influence of changing wellhead pressure is quite straightforward. Decreasing the wellhead pressure will shift the TPR curve downward, resulting in a decrease in rate (Figure 10).

Changing gas liquid ratio

Increasing the gas liquid ratio reduces the hydrostatic pressure loss and increases the friction pressure loss. An increase in the gas liquid ratio will shift the TPR curve upwards and to the right. The result is that the natural flow rate increases first, when it reaches a certain gas liquid ratio, the rate decrease afterwards (Figure 11).

Changing tubing inner diameter

Increasing the inner diameter increases the rate of natural flow rate until a critical diameter is reached. For higher diameters, the rate will decrease. Figure 12 shows the general effect of the tubing inner diameter on the natural flow rate.

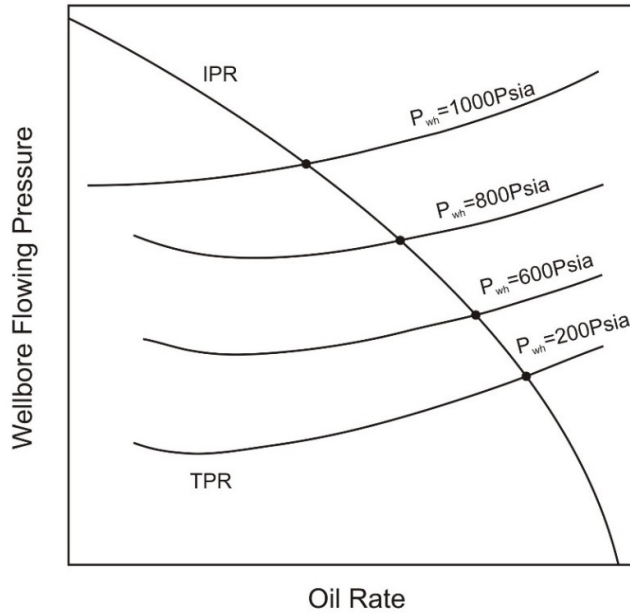


Figure 10 Influence of wellhead pressure on natural flow rate

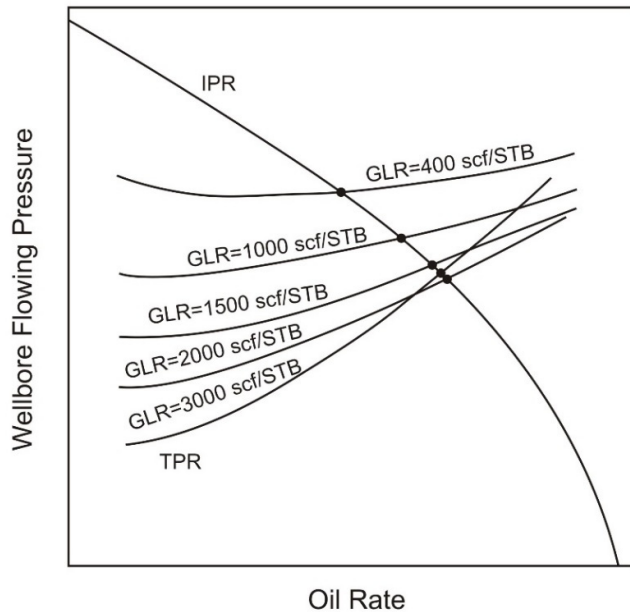


Figure 11 Influence of gas liquid ratio on natural flow rate

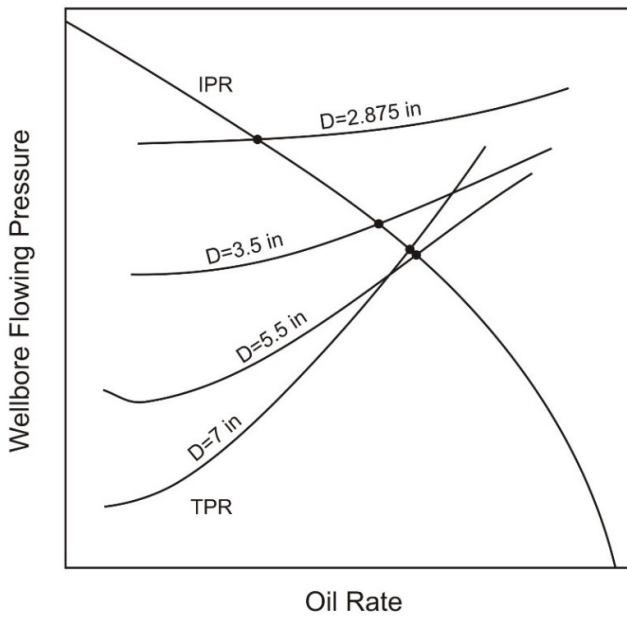


Figure 12 Influence of tubing inner diameter on natural flow rate

Knowing the influence of the well parameters on the natural flow rate will be helpful to take the measures and maintain the expected natural flow rate in the future.

3.5 Application of Material Balance Equation

Once the natural flow rate is obtained, it can be combined with reserves to predict the future reservoir performance by using the material balance equation. The material balance equation was first presented by Schilthuis (1936) and is now one of the fundamental equations used by reservoir engineers for predicting the behavior of hydrocarbon reservoirs. The basic theory of the equation is that if the total observed surface production of oil and gas can be expressed as an underground withdrawal, then this underground withdrawal is equal to the expansion of the fluids in the reservoir resulting from a finite pressure drop. Figure 13 shows the general form of material balance equation.

$$\text{Underground withdrawal} = \text{Expansion of oil and dissolved gas} + \text{Expansion of gas cap} + \text{Reduction in HCPV} + \text{Natural Water Influx}$$

Figure 13 The general form of material balance equation

The equation postulates that the underground withdrawal should be equivalent to the total volume change from the expansion of oil and dissolved gas, the expansion of gas cap, the reduction in hydrocarbon pore volume of the reservoir (HCPV) and the net water influx into the reservoir. The mathematical form of the material balance equation is:

$$N_p(B_o + (R_p - R_s)B_g) = NB_{oi} \left[\frac{(B_o - B_{oi}) + (R_{si} - R_s)B_g}{B_{oi}} + m \left(\frac{B_g}{B_{gi}} - 1 \right) + (1 + m) \left(\frac{c_w S_{wc} + c_f}{1 - S_{wc}} \right) \Delta p \right] + (W_e - W_p)B_w \quad (46)$$

For a gas cap field, it is assumed that the natural water influx is negligible ($W_e = 0$) and, because of the high gas compressibility, the effect of water and pore compressibility is also negligible (Dake, 1983). In this case, the material balance equation can be simplified to:

$$N_p(B_o + (R_p - R_s)B_g) = NB_{oi} \left[\frac{(B_o - B_{oi}) + (R_{si} - R_s)B_g}{B_{oi}} + m \left(\frac{B_g}{B_{gi}} - 1 \right) \right] \quad (47)$$

Based on parameters in the equation above, it is easy to see that N_p and R_p can be derived from the IPR and TPR plots, B_{oi} , B_{gi} and R_{si} can be estimated from PVT correlations at the initial reservoir pressure, and N and m are related to the initial oil and gas in place. Hence, the only thing needed to balance the equation is to find a new reservoir pressure for the B_o , B_g and R_s calculation. Once the new reservoir pressure is obtained, it can be used to generate the new natural flow rate which can be used for balance calculation in the next round. By repeating the processes above, oil and gas production profiles can be generated.

3.6 Model Test and Verification

In the previous sections, the procedures to build the well production model and generate the oil and gas profiles are introduced and discussed in detail. In this section, the model is tested to verify the validity of the well production model and its implementation. The Petroleum Experts software (MBAL, PROSPER and GAP) is used for comparison purposes. The same input parameters are given for both the well production model developed in this work and the Petroleum Experts software.

Initial reservoir pressure	4350 psig
Average reservoir temperature	160°F

Oil API gravity	40°API
Gas gravity	0.7
Oil in place	100MMSTB
Gas cap volume	107.3BSCF
Wellhead pressure	200psig
Wellhead temperature	120°F
Bottomhole temperature	160°F
Well depth	7500ft
Tubing inner diameter	1.995in
Pipe roughness	0.0006in

Table 1 Basic input parameters for model test

We set the production gas-oil ratio equal to the solution gas-oil ratio and the water cut to 0%. The PVT parameters, IPR and TPR curves and the production profiles are generated from both the well production model and the Petroleum Experts software (MBAL, PROSPER, GAP) and the resulting profiles are compared.

PVT parameters verification

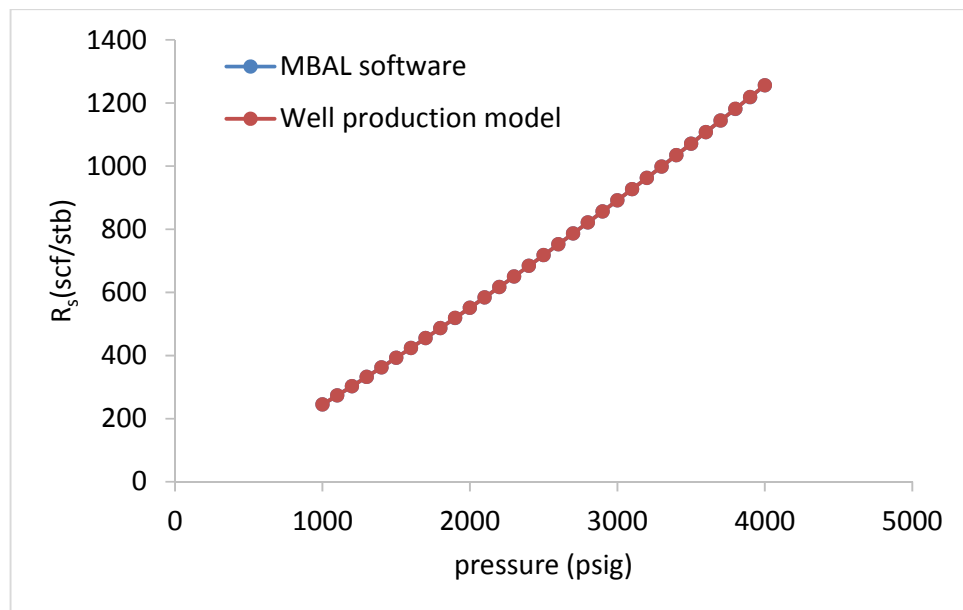


Figure 14 Solution gas oil ratio comparison

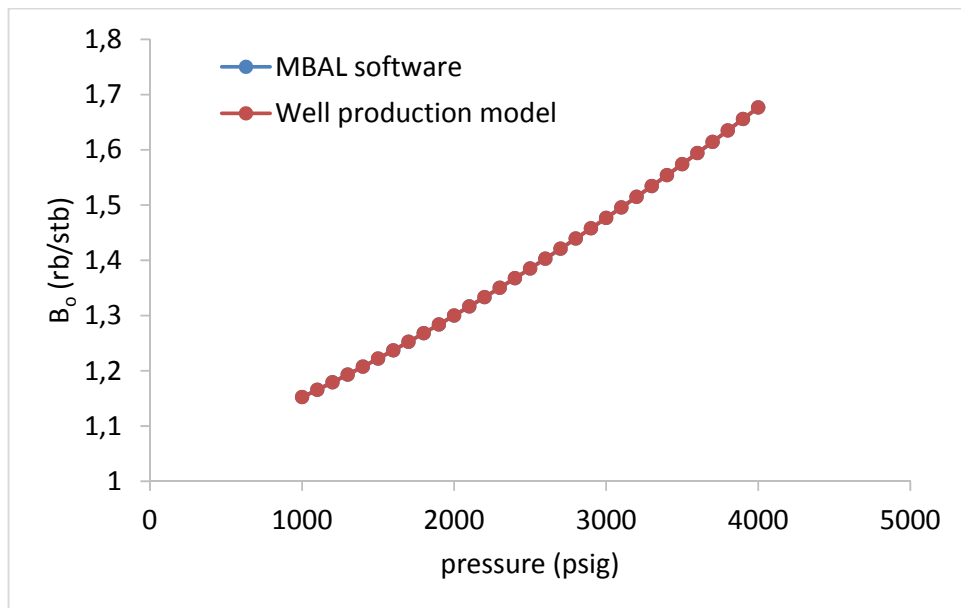


Figure 15 Oil formation volume factor comparison

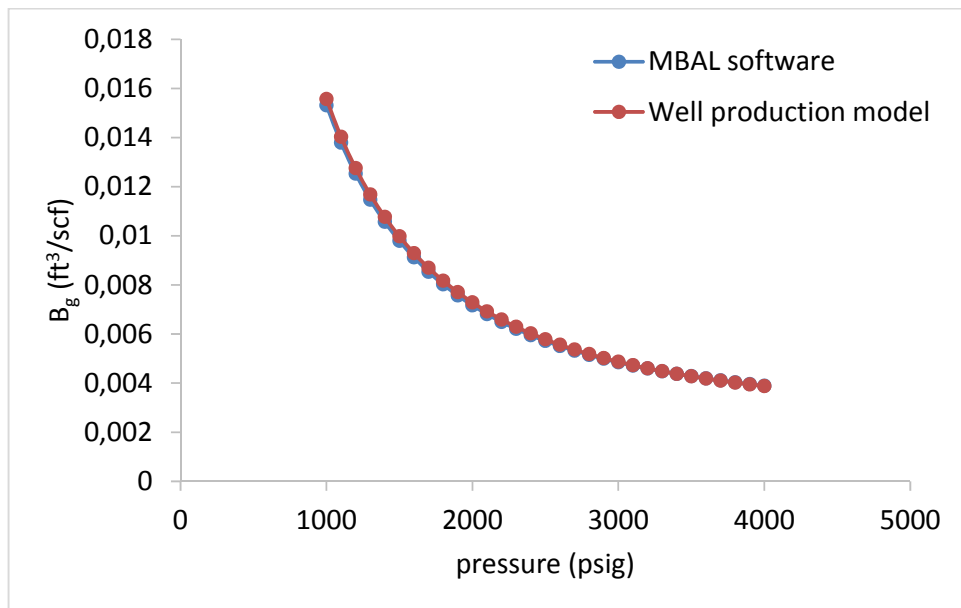


Figure 16 Gas formation volume factor comparison

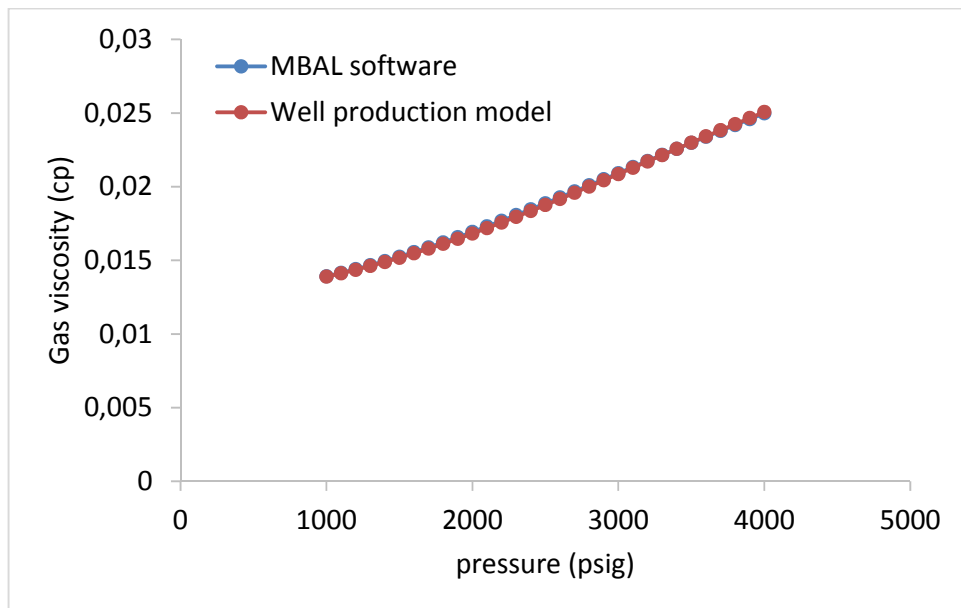


Figure 17 Gas viscosity comparison

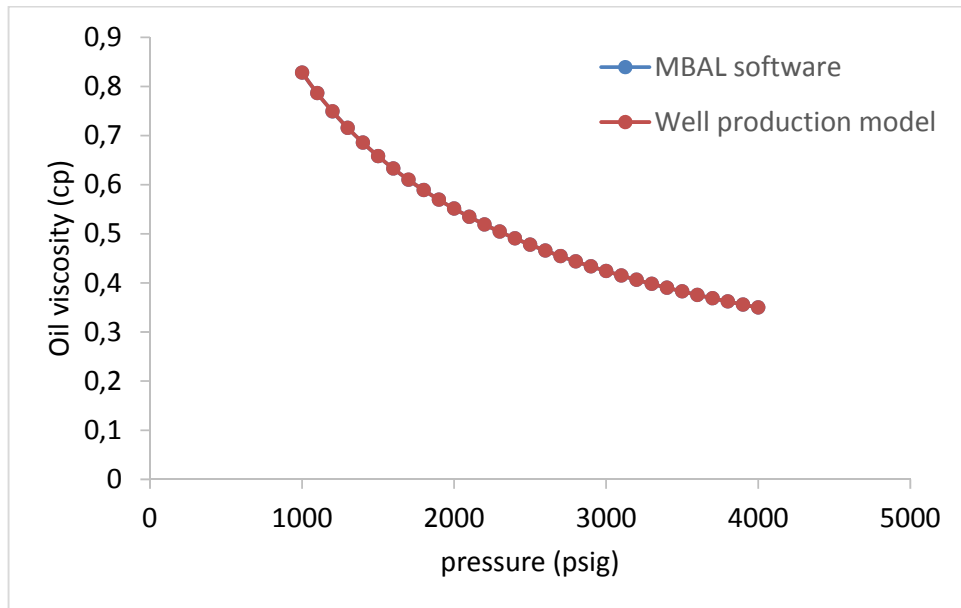


Figure 18 Oil viscosity comparison

Based on the comparison (Figures 14-18), and assuming the Petroleum Experts applications are correct, the average error for solution gas oil ratio R_s , oil formation volume factor B_o , gas formation volume factor B_g , gas viscosity μ_g and oil viscosity μ_o are less than 1%.

IPR and TPR curve verification

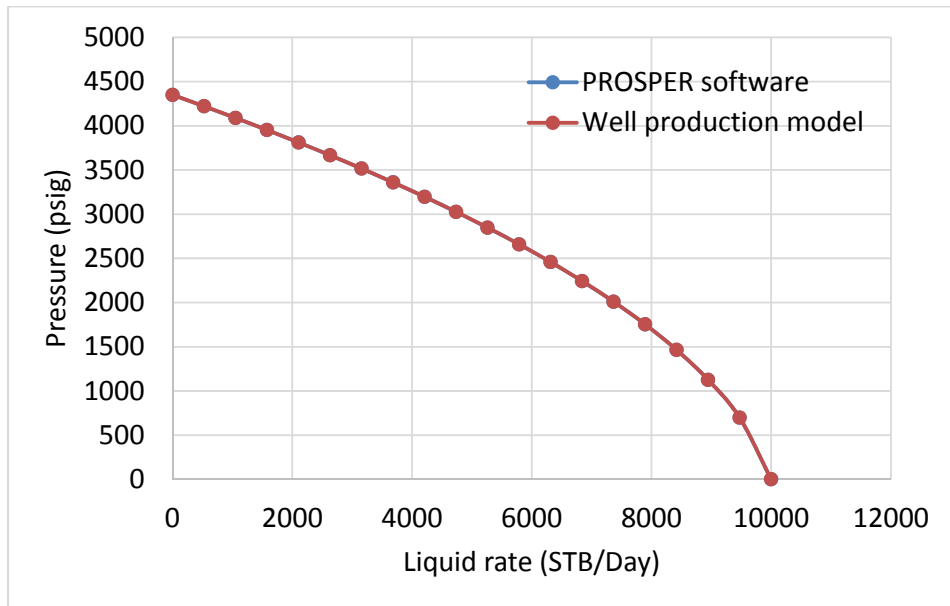


Figure 19 IPR curve comparison

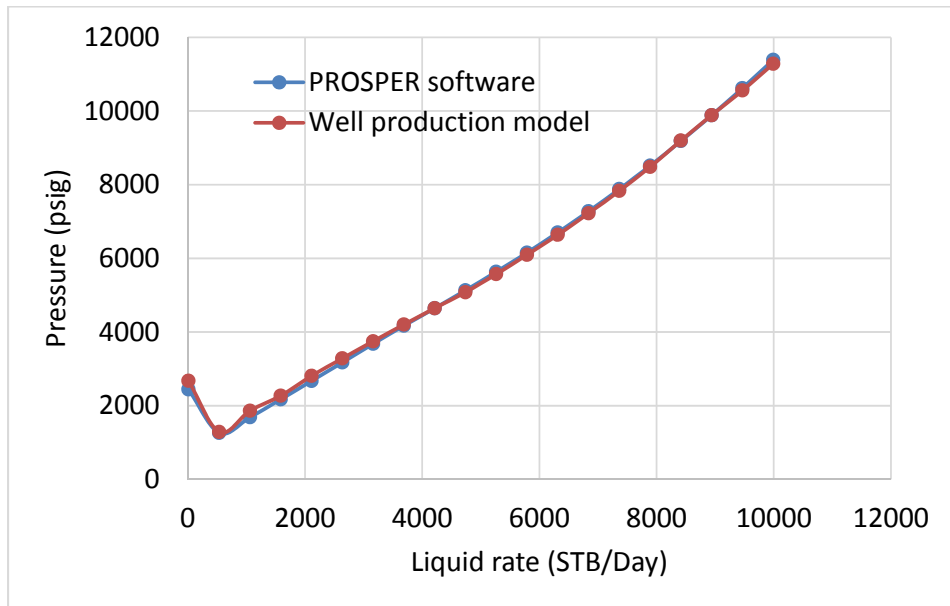


Figure 20 TPR curve comparison

Figures 19 and 20 show IPR and TPR curves calculated from both MBAL software and well production model, the results are quite similar. The average error of IPR and TPR curves is 0.01% and 2.1% respectively.

Production profile verification

The production profile comparison is conducted in two parts. The first part is the oil and gas production profile comparison and the reservoir pressure comparison when the production gas is not reinjected. The second comparison part is the case when the production gas is reinjected to the reservoir.

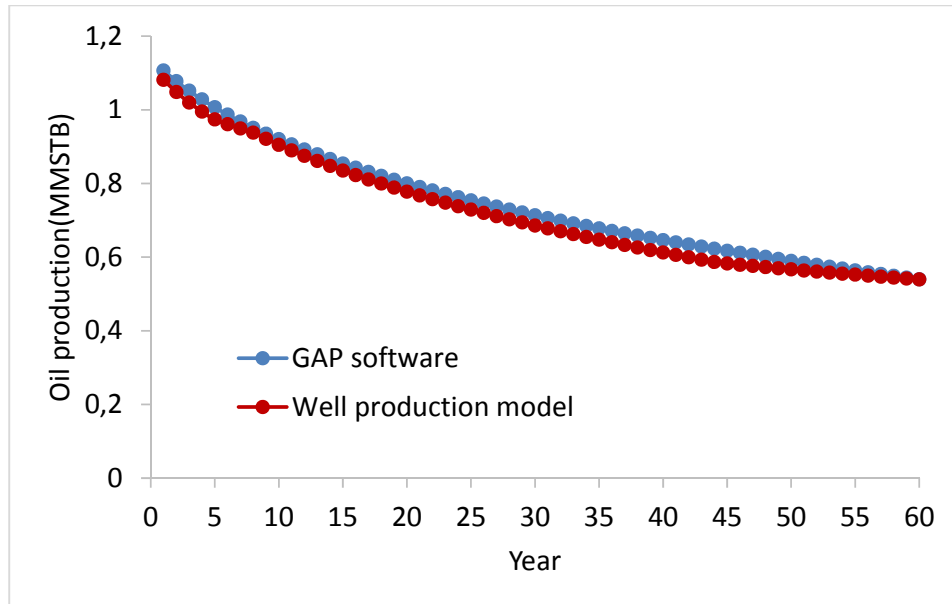


Figure 21 Oil production profile comparison (without gas reinjection)

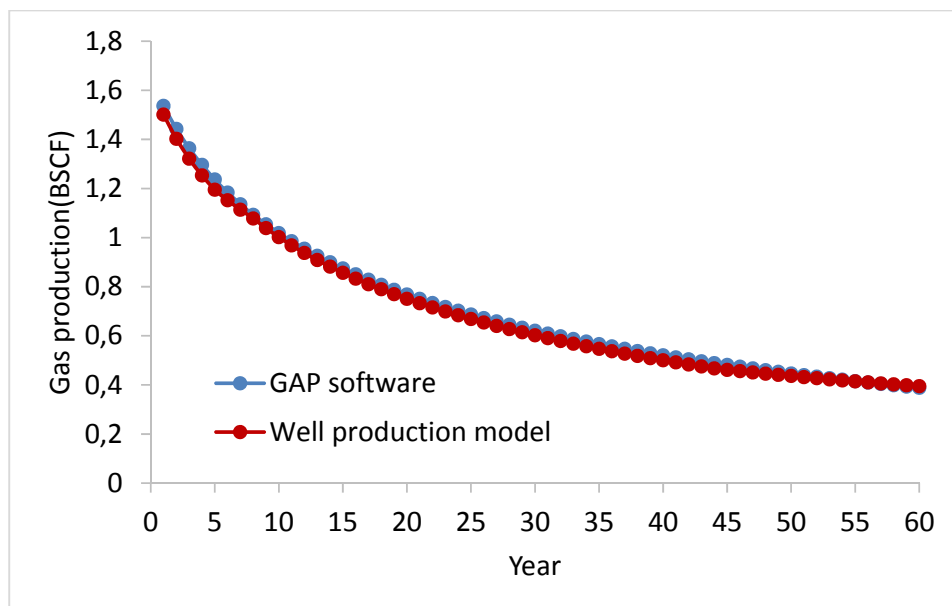


Figure 22 Gas production profile comparison (without gas reinjection)

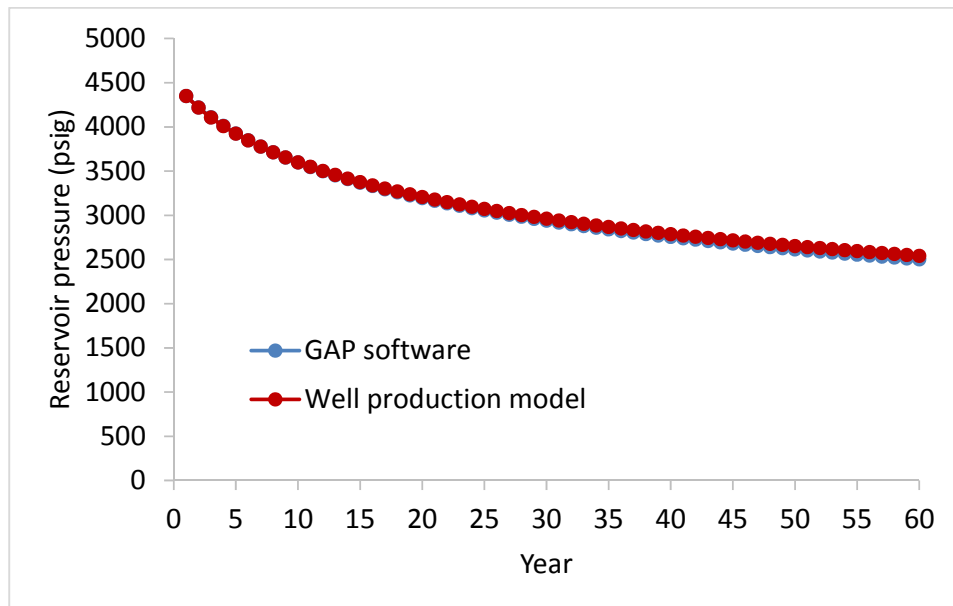


Figure 23 Reservoir pressure declination comparison (without gas reinjection)

Figures above show the oil production profile, gas production profile and reservoir pressure declination respectively when production gas is not reinjected (Figures 21-23). The average error of both oil production and gas production are around 3.1%. The average error of the reservoir pressure is less than 1%.

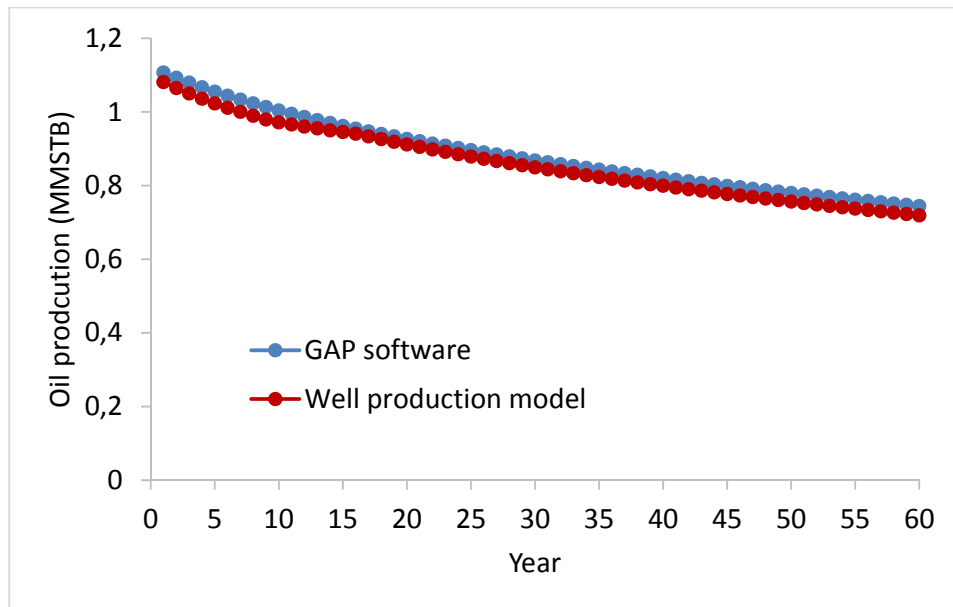


Figure 24 Oil production profile comparison (with gas reinjection)

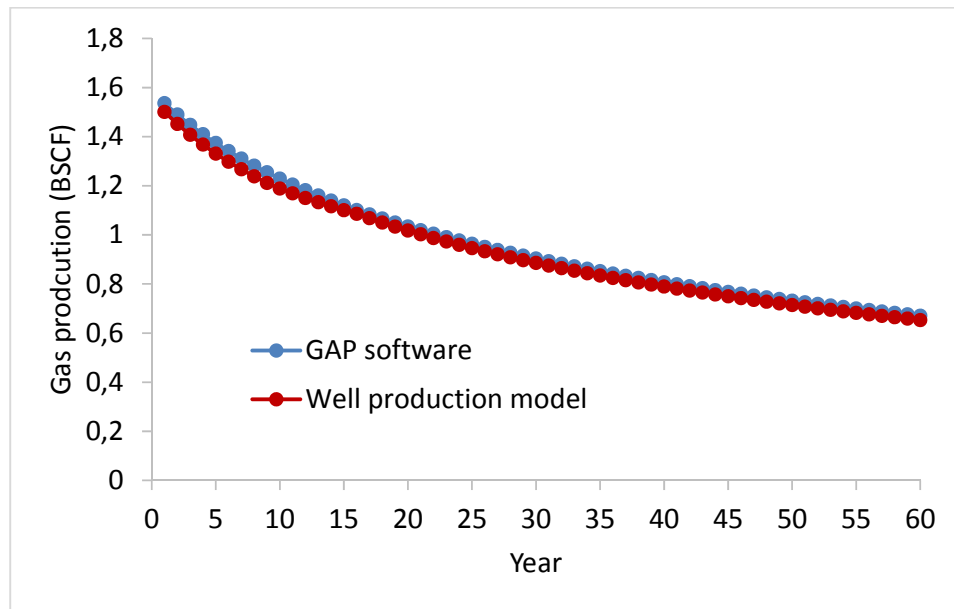


Figure 25 Gas production profile comparison (with gas reinjection)

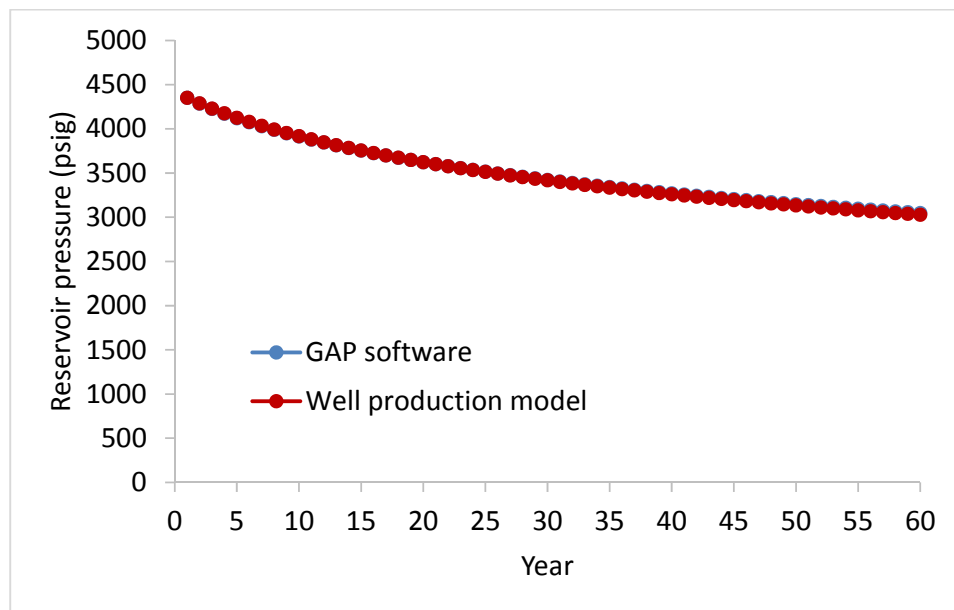


Figure 26 Reservoir pressure declination comparison (with gas reinjection)

Figures 24 to 26 show the oil production profile, gas production profile and reservoir pressure decline when gas reinjection happens. The average error of both oil production and gas production is 2.7% and 2.4% respectively. The average error of reservoir pressure is less than 1%.

Based on the comparisons above, the same trends for the reservoir pressure, oil production and gas production are resulting from both Petroleum Experts software and well production model developed here. The small difference between the results above occur because of different choices of empirical equations for some intermediate variable calculations and the fact that the well production model developed here is not a fully detailed model which can represent the accurate future production. In this study, the goal is to provide sufficient insight to make the best choice clear and not to build the best possible representation of the actual future production. The well production model developed here includes the main characteristics of the production from an oil field with a gas cap and is useful to assess the impact of reserves uncertainty on the oil and gas production.

4. Uncertainty Analysis

In this chapter, the reserves uncertainty and its influence on the oil and gas production will be discussed. The discussion is divided into two parts: 1) the reason why uncertainty occurs and its corresponding distribution; 2) a method to investigate the impact of reserves uncertainty on the oil and gas production.

4.1 Reserves Uncertainty

The reserves estimation in all oil and gas fields includes uncertainty because the evaluation team do never have complete information about the reservoir or of the input parameters required for assessing the oil initially in place and recovery efficiency (RE). A common method to estimate the oil reserves is the volumetric method, it can be expressed as follows:

$$\text{Oil reserves} = A \cdot h \cdot NTG \cdot \phi \cdot (1 - S_w)/B_{oi} \cdot RE \quad (48)$$

From this equation, we see that the porosity is one of the input parameters. But the porosities determined from the well data do not provide perfect information of the porosity of the entire field. Hence, geologists have to estimate the distribution of the porosity for the whole field by their expert knowledge and experience. The same situation applies to the assessment of other parameters. Once the experts have assessed the uncertainty for each of the input parameters, the reserves uncertainty can be calculated by repeatedly sampling these distributions and calculating the reserves. By central limit theorem, the product of independent random variable approaches a lognormal distribution. Therefore, the distribution of oil and gas reserves calculated by equation (48) with uncertain input parameters will be lognormal regardless of the distribution used for the input variables (Demirmen, 2007). In this study, the PERT distribution is chosen to represent the reserves, because it provides a reasonable approximation of the lognormal distribution and because the parameters required to specify the PERT distribution often are easier to assess than the mean and standard deviation required for the lognormal distribution. The PERT distribution can be defined by different sets of three points. It could be the minimum (a), mode (b) and maximum (c) or, say, the P10, P50 and P90. If the min, mode and max are used, it is easy to calculate mean μ and standard deviation σ of this distribution.

$$\text{mean } \mu = \frac{a + 4b + c}{6} \quad (49)$$

$$\text{Standard deviation } \sigma = \frac{c - a}{6} \quad (50)$$

The flexibility of the PERT distribution is demonstrated in Figure 27 with three distributions with different minima (a), modes (b) and maxima (c). The flexibility in choosing input parameters for which the expert has some intuition, such as the percentiles, makes it easy to update the distribution as new knowledge is obtained.

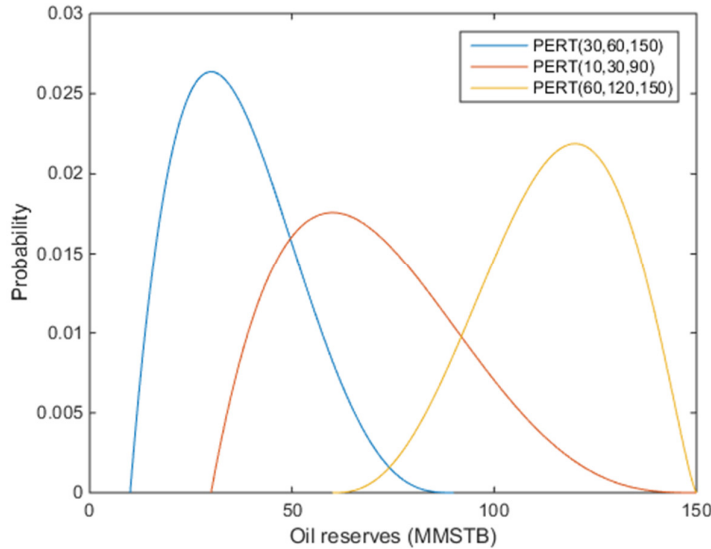


Figure 27 Three PERT distributions with different input parameters

4.2 Monte Carlo Simulation

Monte Carlo simulation (MCS) is a mathematical technique that makes it practical and relatively easy to aggregate and quantify uncertainty and to investigate the impact of uncertainty on decision alternatives. The result of a MCS is a range of possibilities with associated probabilities; i.e., a probability distribution of the variable of interest. MCS is commonly used in the oil and gas industry, for example to estimate the hydrocarbon reserves in place (Bratvold and Begg, 2010). In this work, MCS is combined with the well production model to assess the impact of reserves uncertainty on oil and gas production.

Figure 28 illustrates the general procedure of MCS with two input parameters. First, for each input variable, MCS samples from the probability distribution. Then, the samples are used in the model or function to calculate the output variables. The result is stored and the previous steps are repeated a large number of times. The result of a MCS are distributions of the variables of interest (OOIP, GIIP, reserves, production, NPV, etc.).

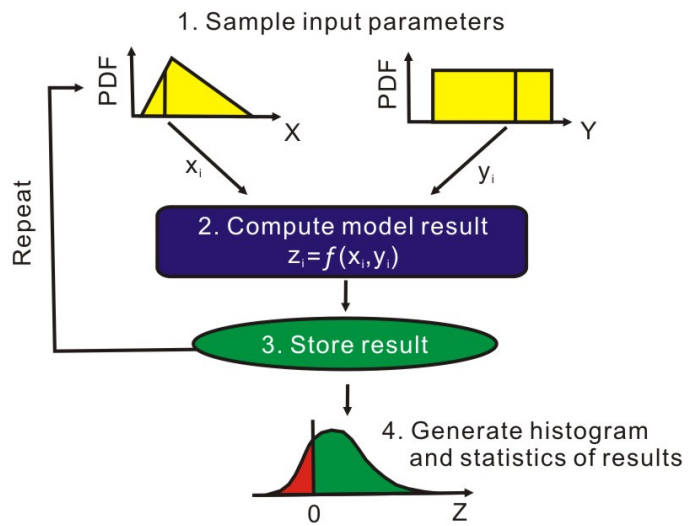


Figure 28 The general procedures of Monte Carlo simulation (Bratvold and Begg, 2010)

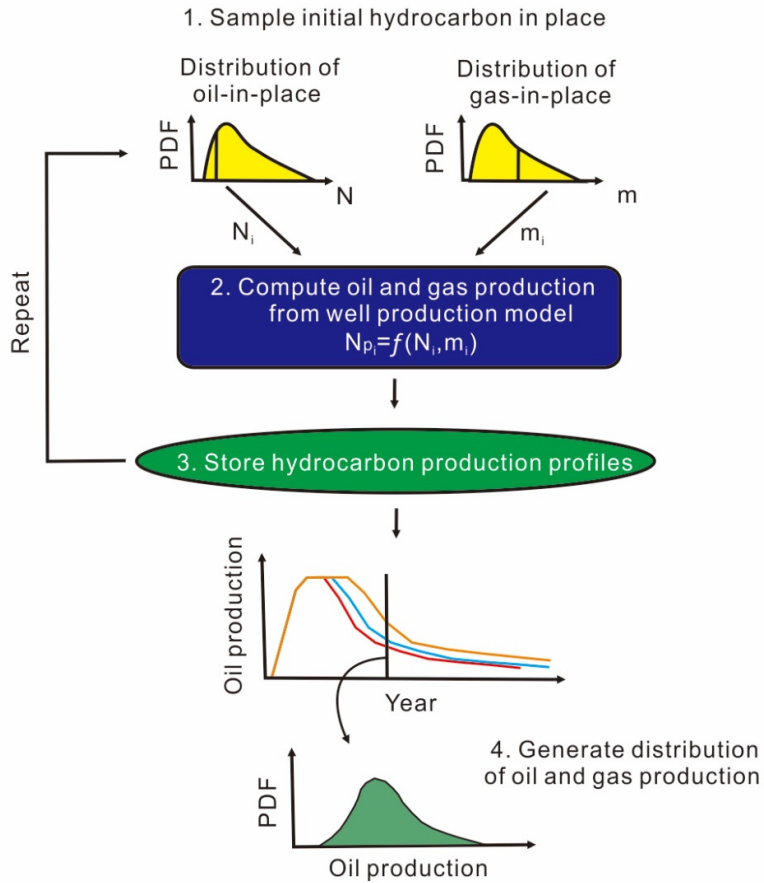


Figure 29 The procedures of Monte Carlo simulation in this study

In this study, we apply MCS to assess the impact of the reserves uncertainty on the oil and gas production. Figure 29 shows the MCS procedure for this specific case. First, the probability distributions for oil and gas in place are being sampled. Then the sampled oil and gas in place are used in the well production model to generate a single realization of oil and gas production profiles. The oil and gas production profiles are stored and the input distributions are sampled and used to generate for new realizations of the production profiles. All the realizations of the production profiles are stored and the end result is a distribution of possible oil and gas productions at a given point in time. Not only does the procedure provide the range of possibilities, it also furnish probabilities of all the possibilities.

4.3 A Case Study

In order to understand how the oil and gas reserves influence the oil and gas production, a case study was developed for the X gas cap field. The estimated distribution of initial hydrocarbon in place in the X are listed below (Table 2). 20 production wells have been drilled to produce oil, and the produced solution gas is reinjected into the reservoir. Due to limitations in the capabilities of installed infrastructure and pipelines, the oil production is constrained to a maximum rate of 360,000 STB/Day. The maximum oil production rate is expected to be achieved in 6th year after production is started.

	Minimum (a)	Mode (b)	Maximum (c)
Initial oil in place (N)	2000 MMSTB	4000 MMSTB	15000 MMSTB
gas cap-to-oil volume ratio (m)	0.2	0.4	1.2

Table 2 Distribution of initial hydrocarbon in place in X gas cap field

The required input parameters for predicting oil and gas production are listed below (Table 3).

Initial reservoir pressure	4263psig
Average reservoir temperature	180°F
Oil API gravity	38.5°API
Gas gravity	0.62
Wellhead pressure	650psig
Wellhead temperature	120°F
Bottomhole temperature	180°F
Well depth	8200ft

Tubing inner diameter	5.5in
Pipe roughness	0.0006in

Table 3 Basic input parameters in the X gas cap field

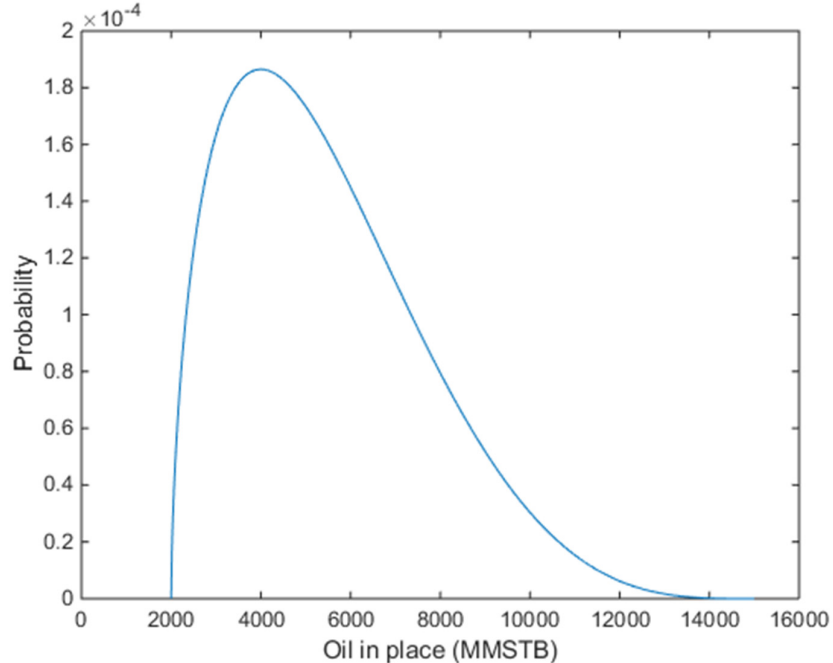


Figure 30 The probability distribution of oil in place

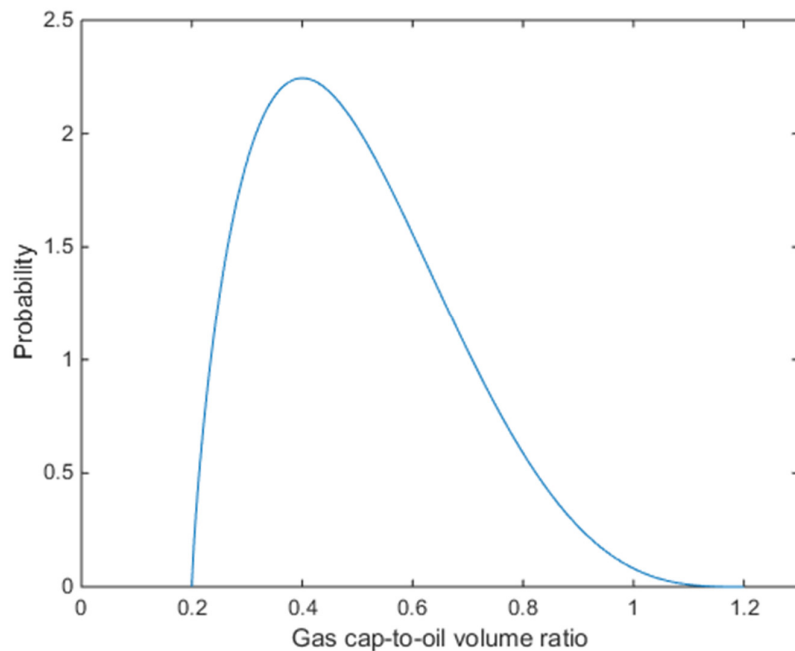


Figure 31 The probability distribution of gas cap-to-oil volume ratio

PERT distributions for oil in place and gas cap-to-oil volume ratio were generated using minimum, mode and maximum values supplied by the geoscientists (Figures 30 and 31). Once the input uncertainties have been assessed, the MCS procedure is used to generate the oil and gas production profiles.

Before running Monte Carlo simulation, an important question which needs to be addressed is the number of iterations to use in the MCS. By the law of large numbers, the errors in a MCS goes to zero as the number of iterations goes to infinity. Thus, in deciding on the number of iterations there are two opposing considerations: 1) too few iterations leads to inaccurate outputs and 2) too many iterations leads to large computational costs and long simulation times. As a rule of thumb, the following order-of-magnitude guidelines for the number of iterations are listed by Yoe (2011):

- Determining the mean of results - 10^2
- Estimating outcome probabilities - 10^3
- Defining tails of output distribution - 10^4

In this study, some plots are generated to help to decide on the number of iterations. Figure 32 and 33 show the comparison of the mean and standard deviation from original oil in place distribution and the samples. It can be observed that the mean and standard deviation of the samples are fluctuant when the number of iteration are less than 1000, but both values become stable and are close to the values calculated from the original oil in place distribution when the number of iteration are equal to or larger than 1000. In this case, the mean of oil in place distribution is 5500 MMSTB and the standard deviation of oil in place distribution is 2166.7.

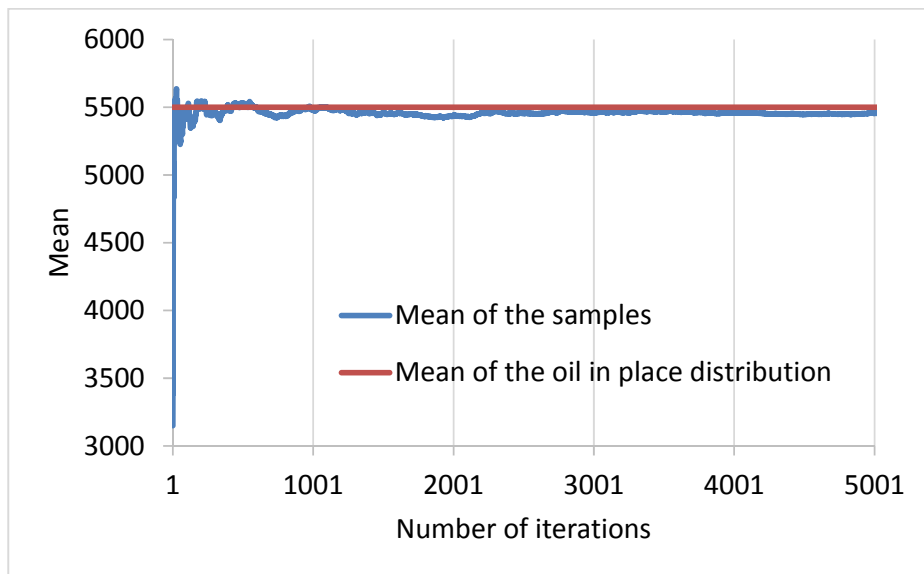


Figure 32 Running average of samples from oil in place distribution

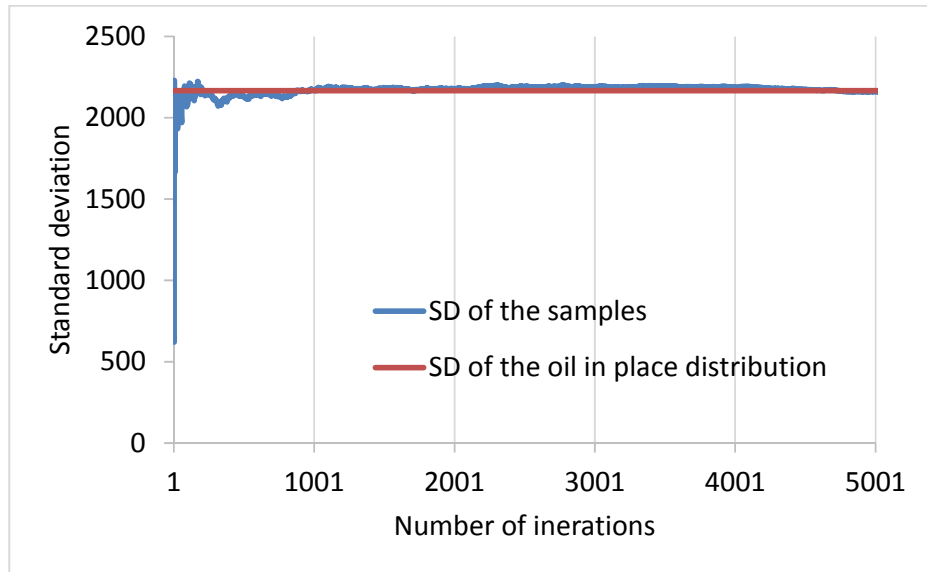


Figure 33 Running standard deviation of samples from oil in place distribution

The computational time for different number of iterations in this simulation are also tested to help make this decision (Figure 34). A linear relationship between the number of iterations and its corresponding computational time can be observed. It takes 8-9 hours to run 1000 iterations, so it can be speculated that it may take 80-90 hours to run 10000 iterations. Hence, considering the guidelines above, the observations from plots and the time limitation, 1000 iterations are performed to estimate the influence of reserves uncertainty on oil and gas production in this study.

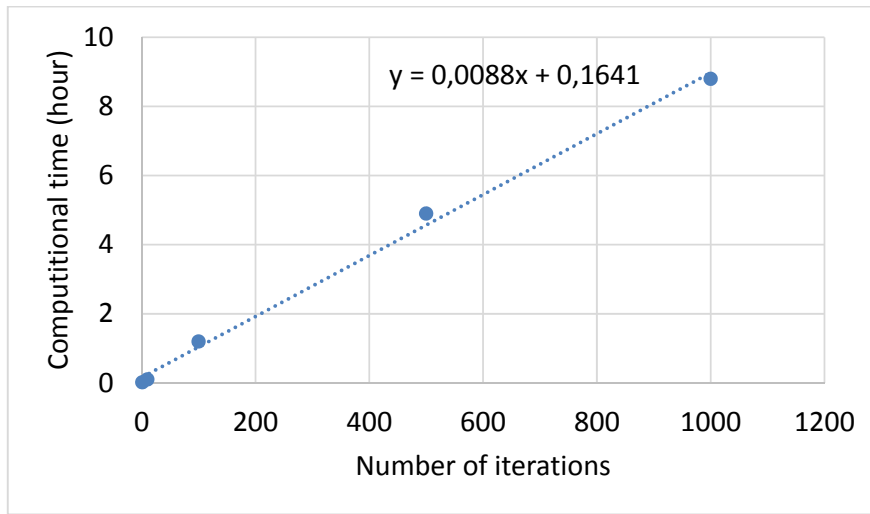


Figure 34 The number of iterations and its corresponding computational time

With 1000 iterations, 1000 possible oil and gas production profiles are generated (Figure 35). The thick black line in Figure 35 is the mean production of these 1000 oil production profiles. We can now examine how the oil and gas reserves influence the oil and gas production.

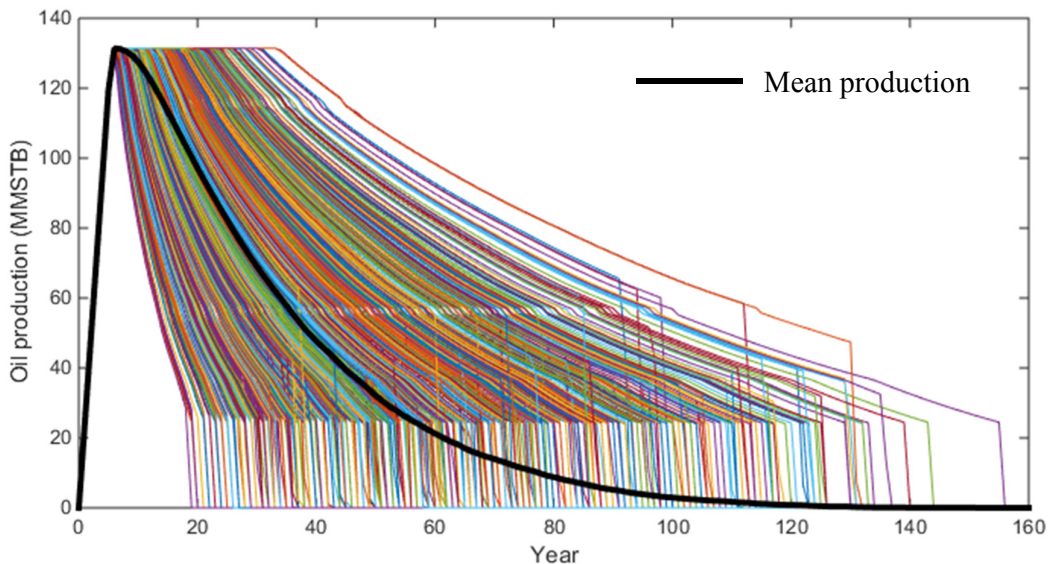


Figure 35 Oil production profiles generated from 1000 iterations and its mean production profile

Since both the oil in place and gas cap-to-oil volume ratio have an effect on the oil and gas production, 3D plots are generated to show the relationship between oil and gas in place and oil production for different production years (Figure 36). It can be observed that the oil production data can be divided into two parts. The first part is the data with zero production—the “floor” in the graph, which means that the production wells stop producing oil at that specific year as a function of the corresponding oil and gas in place. The other part is the production data with values larger than zero which means that the wells are producing. The data from the producing part fall on surfaces in the 3D plot. Hence, the surface trend analysis is performed to look for this relationship.

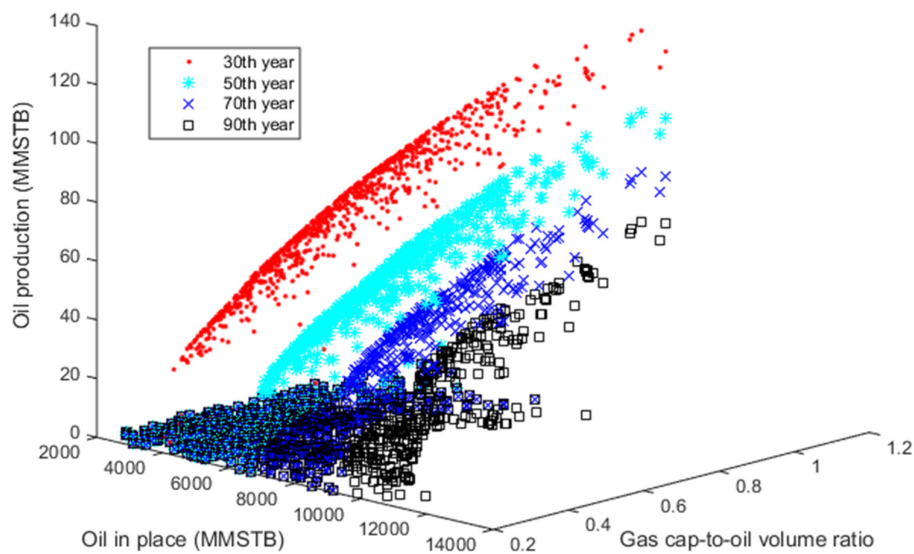


Figure 36 The relationship between oil and gas in place and oil production at four different years

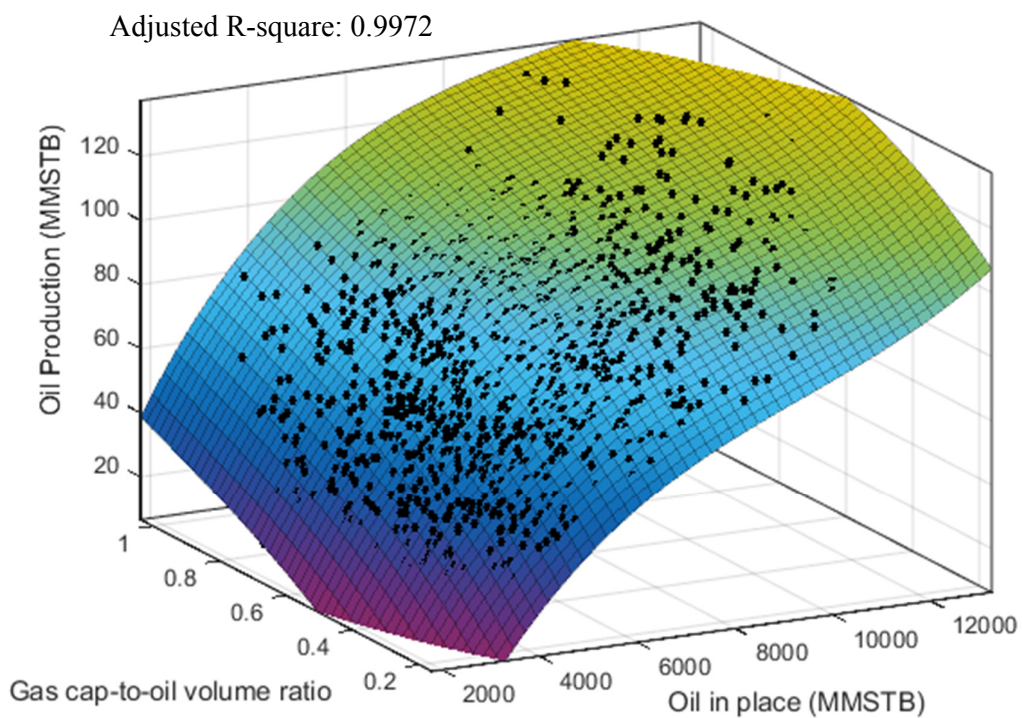


Figure 37 The trend surface analysis for oil production at the 30th year

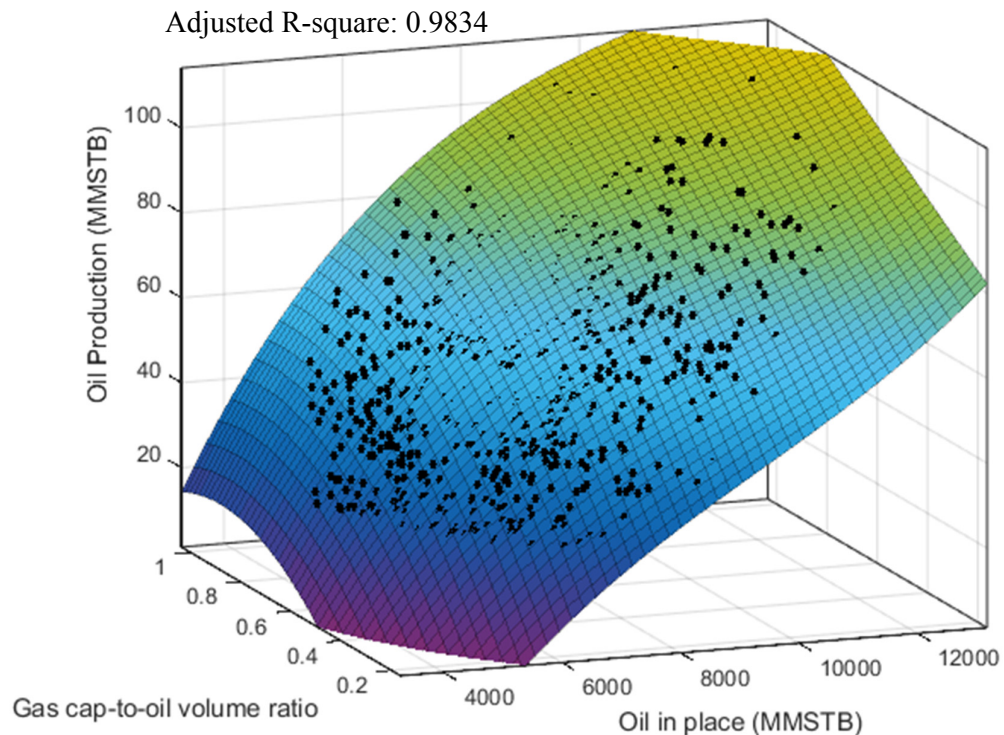


Figure 38 The trend surface analysis for oil production at the 50th year

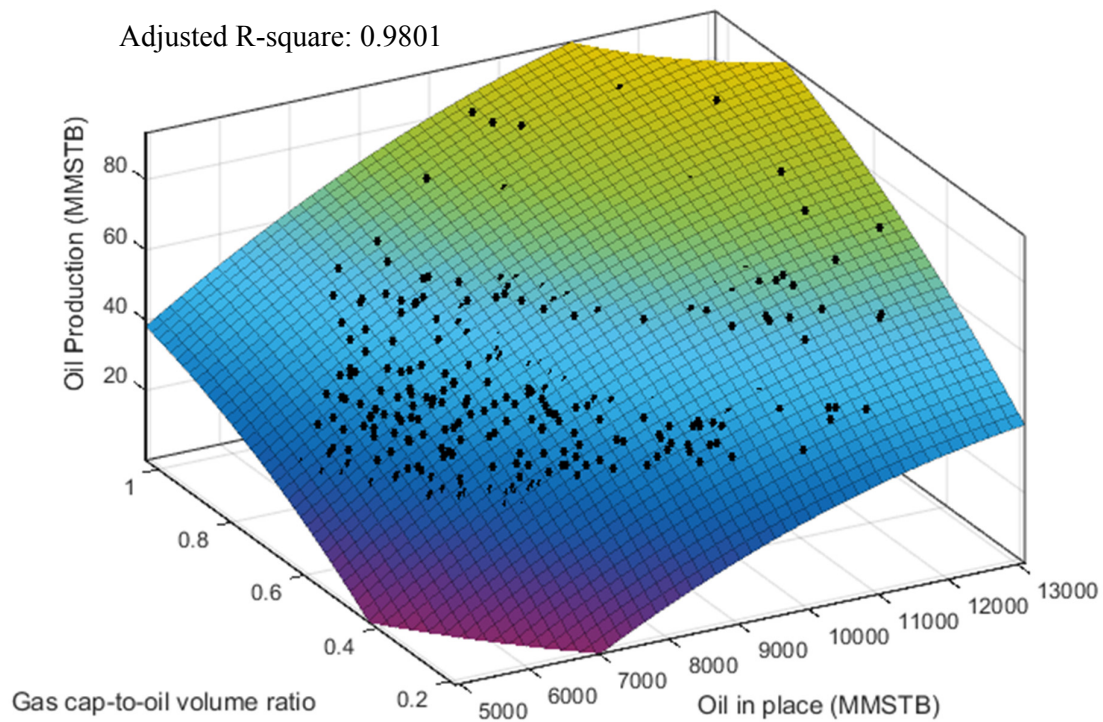


Figure 39 The trend surface analysis for oil production at the 70th year

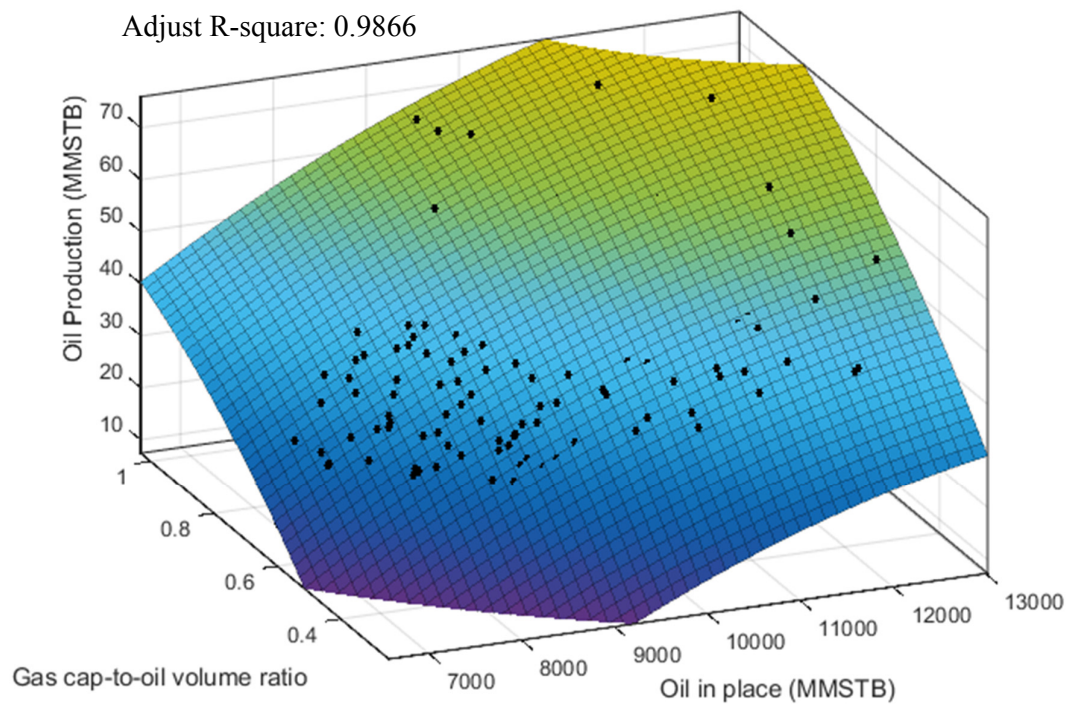


Figure 40 The trend surface analysis for oil production at the 90th year

Trend surface analysis is a global surface-fitting technique. The mapped data are approximated by a polynomial expansion. Figures 37-40 display the surface trends based on oil in place, gas cap-to-oil volume ratio and oil production at four different production years. The goodness of fit of the multiple regression model can be assessed by the adjusted R-square. The adjusted R-square can take on any value less than or equal to 1, with a value closer to 1 indicating a better fit. The adjusted R-square values above are all larger than 0.98 which indicate a good fit. Therefore, a mathematical expression could be used to describe the relationship between oil in place, gas cap-to-oil volume ratio and oil production and predict the oil production at each production year. For example, the oil production for the 70th year in this case can be predicted by the following equation:

$$z = -124.8 + 0.01866x + 140.5y - 5.769 * 10^{-7}x^2 - 0.001038xy - 47.19y^2 \quad (51)$$

where x is the initial oil in place, y is the initial gas cap-to-oil volume ratio and z is the corresponding oil production at the 70th year. Hence, this equation can be used to predict oil production at the 70th year in this specific case with any combination of the initial oil in place (x) and the initial gas cap-to-oil volume ratio (y). At another production year, another mathematical equation can be constructed based on the oil production profiles generated from iterative computation and used for oil production prediction at that specific year.

In order to further study the influence of oil and gas in place on oil and gas production, the oil and gas production profiles generated from the new distributions of hydrocarbon in place are compared with the previous oil and gas production profiles. The new distributions of hydrocarbon in place are obtained by shifting the mode of previous distributions 25% to the left and right respectively (Figure 41 and 42). The middle distributions with red color in the following graphs are the previous distributions for oil in place and gas cap-to oil volume ratio. The same procedures of MCS are used for the new distributions to generate the oil and gas production profiles. In order to compare the difference, the average oil production is selected as the decision criterion. Then the average oil productions at the specific years resulting from the new oil production profiles are calculated and used to perform a sensitivity analysis. In the tornado charts below (Figure 43), the vertical black line close to the middle of each chart represents the average oil production from the original distributions of oil in place and gas cap-to-oil volume ratio. The green and red areas represent the average oil production from the shifted distribution of oil in place and gas cap-to-oil volume ratio. The green areas indicate the 25% left shift from the mode value of the original distributions and the red areas indicate the

25% right shift from the mode value of the original distributions. The tornado charts show that the oil production is more sensitive to changes in oil in place than gas cap-to-oil volume ratio.

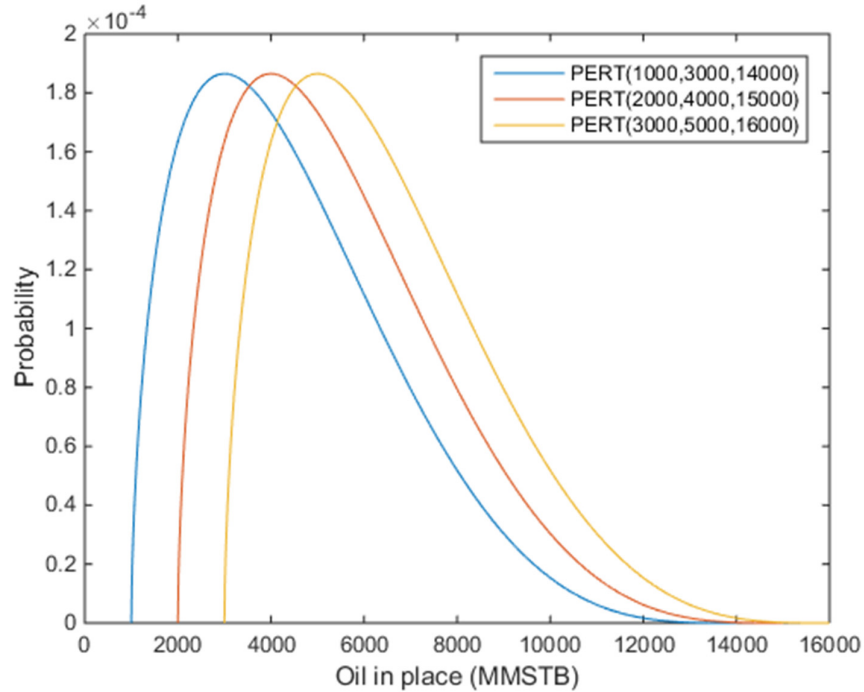


Figure 41 The shifted and original distributions of oil in place

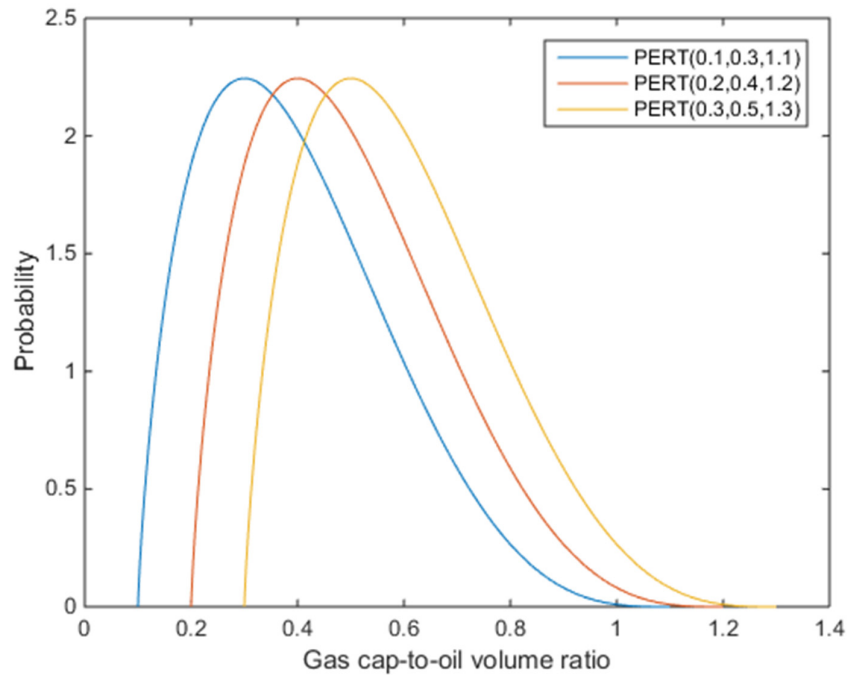


Figure 42 The shifted and original distributions of gas cap-to-oil volume ratio

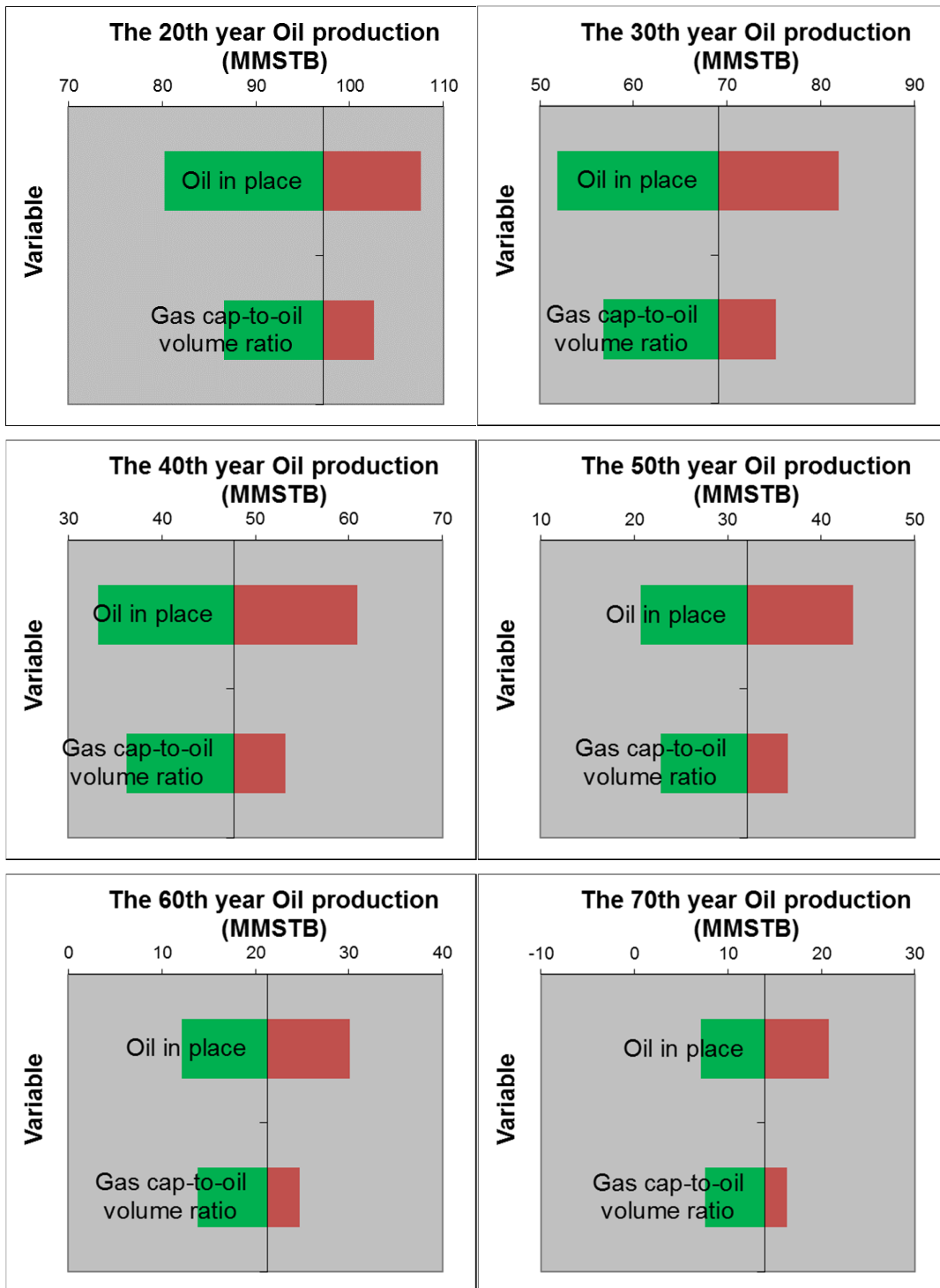


Figure 43 The tornado chart to identify the main uncertainty driver

The recoverable oil reserves; i.e., the total oil production can be obtained by summing each oil production profile. By combining the reserves with the oil in place, the recovery efficiency can be calculated for each realization. Figure 44 is a scatterplot of oil recovery efficiency versus oil in place and Figure 45 shows the recovery efficiency versus gas cap-to-oil volume ratio.

The scatterplot in Figure 44 indicates no obvious relationship between oil in place and oil recovery efficiency. However, Figure 45 exhibits a strong relationship between gas cap-to-oil volume ratio and oil recovery efficiency. A critical gas cap-to-oil volume ratio can be identified as well in this case. When the ratio is equal or larger than 0.67, the recovery efficiency is 100%. When the ratio is less than 0.67, a linear relationship between gas cap-to-oil volume ratio and oil recovery efficiency can be observed. Since the model is a simplified model that does not include the geological factors that can influence the recovery efficiency, such as porosity, permeability and reservoir connectivity, the oil recovery efficiency here is higher than a real situation and shows a linear relationship with gas cap-to-oil volume ratio. However, it still reflects that gas cap volume is the main factor that influences the oil recovery efficiency. Further work could be done to investigate the relationship between gas cap-to-oil volume ratio and oil recovery efficiency in other cases with different input parameters, and then to examine if there are any connection between the critical gas cap-to-oil volume ratios in different cases.

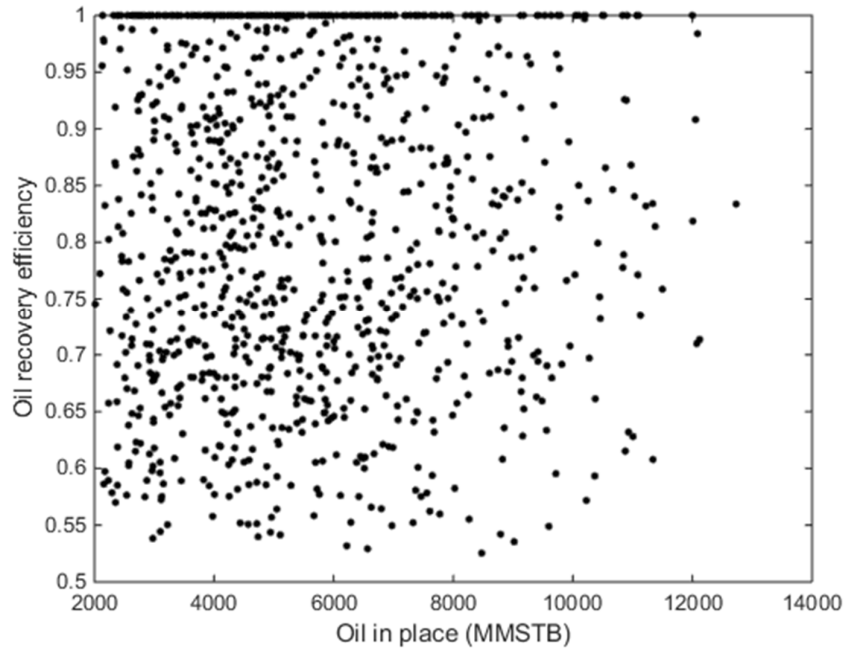


Figure 44 The relationship between oil in place and recovery efficiency

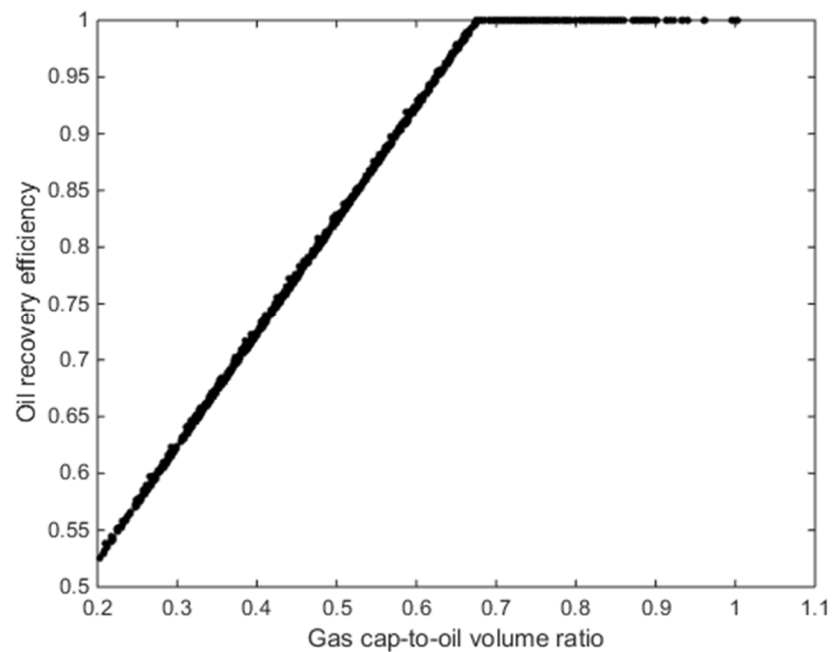


Figure 45 The relationship between gas cap-to-oil volume ratio and recovery efficiency

5. Discussion and Conclusion

In this study, an approach to assess the impact of reserves uncertainty on oil and gas production for gas cap fields has been introduced, implemented and discussed. The inflow performance relationship (IPR) and tubing performance relationship (TPR) curves used to generate the natural flow rate. The natural flow rate is combined with the material balance equation to construct a well production model to generate oil and gas production profiles, which is the core of this approach.

The conventional methods to predict the oil and gas production are computationally expensive as the production models often are based on a highly detailed model utilizing a large number of grid cells. The high computational cost makes these production models unfeasible for probabilistic analysis and decision support under uncertainty.

Unlike conventional methods, the approach discussed here provides a compelling and efficient way to generate oil and gas production profiles that encapsulates the uncertainty, or lack of knowledge, of the geoscientists and reservoir engineers. Using Monte Carlo simulation, volumetric and reserves uncertainties can be combined with the production model to (1) generate production time-series with uncertainties and (2) to assess the impact of reserves uncertainties on the oil and gas production profiles. The end purpose of such assessing and quantifying these uncertainties is to support reservoir management decisions.

The modeling approach is applied to X gas cap field to assess the impact of reserves uncertainty on oil and gas production. Some general conclusions can be reached based on the case results. First, a simple functional form can be used as a good approximation for the relationship between oil in place, gas cap-to-oil volume ratio and oil production at each production year. This functional form can then be used to predict the oil production. Second, the uncertainty in oil in place has a larger impact on the oil production than the uncertainty in gas in place. Thus, if it is important to reduce the uncertainty in the oil production, the main effort should be reducing uncertainty in oil in place. Finally, the gas cap volume is the main factor which impacts the oil recovery efficiency.

In addition to the application of the discussed production model in this thesis, it has also applied to another, parallel, master thesis project “Depressurization of Oil Fields with Gas Injection”. In that project, we have applied the approach to an example gas cap field to generate oil and gas production profiles at different blowdown (depressurization) times, which provides insights to the decision situation concerning optimal timing for blowdown.

Though this approach has advantages, it is not a general replacement of traditional production prediction techniques. The purpose of developing the production model discussed in this thesis is to provide decision makers with a cogent and tractable means of predicting future oil and gas production with uncertain reserves and support reservoir management decisions.

References

- Abdul-Majeed, G.H., Al-Soof, N.B.A., 2000. Estimation of gas–oil surface tension. *Journal of Petroleum Science and Engineering*, 27(3): 197-200.
- Al-Marhoun, M.A., 1988. PVT correlations for Middle East crude oils. *Journal of Petroleum Technology*, 40(05): 650-666.
- Beggs, D.H., Brill, J.P., 1973. A study of two-phase flow in inclined pipes. *Journal of Petroleum technology*, 25(05): 607-617.
- Beggs, H.D., Robinson, J., 1975. Estimating the viscosity of crude oil systems. *Journal of Petroleum technology*, 27(09): 140-141.
- Bratvold, R., Begg, S., 2010. Making good decisions. Society of Petroleum Engineers.
- Dake, L.P., 1983. Fundamentals of reservoir engineering, 8. Elsevier.
- Demirmen, F., 2007. Reserves estimation: the challenge for the industry. *Journal of Petroleum Technology*, 59(05): 80-89.
- Dranchuk, P., Abou-Kassem, H., 1975. Calculation of Z factors for natural gases using equations of state. *Journal of Canadian Petroleum Technology*, 14(03).
- Duns, H., Ros, N., 1963. Vertical flow of gas and liquid mixtures in wells, 6th World Petroleum Congress. World Petroleum Congress.
- Eickmeier, J.R., 1968. How to Accurately Predict Future Well Productivities. *World Oil*, 99.
- Fetkovich, M., 1973. The isochronal testing of oil wells, Fall Meeting of the Society of Petroleum Engineers of AIME. Society of Petroleum Engineers.
- Glaso, O., 1980. Generalized pressure-volume-temperature correlations. *Journal of Petroleum Technology*, 32(05): 785-795.
- Golan, M., Whitson, C.H., 1991. Well performance. Prentice Hall.
- Guo, B., Lyons, W.C., Ghalambor, A., 2011. Petroleum production engineering, a computer-assisted approach. Gulf Professional Publishing.
- Hagedorn, A.R., Brown, K.E., 1965. Experimental study of pressure gradients occurring during continuous two-phase flow in small-diameter vertical conduits. *Journal of Petroleum Technology*, 17(04): 475-484.
- Hall, K.R., Yarborough, L., 1973. A new equation of state for Z-factor calculations. *Oil and Gas journal*, 71(25): 82-92.
- Hasan, A., Kabir, C., 1992. Two-phase flow in vertical and inclined annuli. *International Journal of Multiphase Flow*, 18(2): 279-293.
- Hough, E., Rzasa, M., Wood, B., 1951. Interfacial tensions at reservoir pressures and temperatures; apparatus and the water-methane system. *Journal of Petroleum Technology*, 3(02): 57-60.
- Katz, D.L.V., 1959. Handbook of natural gas engineering. McGraw-Hill.
- Lasater, J., 1958. Bubble point pressure correlation. *Journal of Petroleum Technology*, 10(05): 65-67.
- Lee, A.L., Gonzalez, M.H., Eakin, B.E., 1966. The viscosity of natural gases. *Journal of Petroleum Technology*, 18(08): 997-1,000.
- Orkiszewski, J., 1967. Predicting two-phase pressure drops in vertical pipe. *Journal of Petroleum Technology*, 19(06): 829-838.
- Petrosky Jr, G., Farshad, F., 1993. Pressure-volume-temperature correlations for Gulf of Mexico crude oils, SPE annual technical conference and exhibition. Society of Petroleum Engineers.
- Rawlins, E.L., Schellhardt, M.A., 1935. Back-pressure data on natural-gas wells and their application to production practices, Bureau of Mines, Bartlesville, Okla.(USA).
- Schilthuis, R.J., 1936. Active oil and reservoir energy. *Transactions of the AIME*, 118(01): 33-52.

- Selley, R.C., Sonnenberg, S.A., 2014. Elements of petroleum geology. Academic Press.
- Standing, M., 1947. A pressure-volume-temperature correlation for mixtures of California oils and gases, Drilling and Production Practice. American Petroleum Institute.
- Standing, M.B., Katz, D.L., 1942. Density of natural gases. Transactions of the AIME, 146(01): 140-149.
- Sutton, R., 1985. Compressibility factors for high-molecular-weight reservoir gases, SPE Annual Technical Conference and Exhibition. Society of Petroleum Engineers.
- Thomas, P., Bratvold, R.B., 2015. A Real Options Approach to the Gas Blowdown Decision, SPE Annual Technical Conference and Exhibition. Society of Petroleum Engineers.
- Vazquez, M., Beggs, H.D., 1980. Correlations for fluid physical property prediction. Journal of Petroleum Technology, 32(06): 968-970.
- Vogel, J., 1968. Inflow performance relationships for solution-gas drive wells. Journal of petroleum technology, 20(01): 83-92.
- Yoe, C., 2011. Principles of risk analysis: decision making under uncertainty. CRC press.

Appendices

Appendix A: MATLAB code for pressure drop calculation

```
function [ PDTrue ] = PressureDroptest(RP,OilR,InsD,WHP,PD) % Pressure Drop Calculation
% Summary of this function goes here
% To calculate the pressure drop along the production tubing by using Beggs and Brill correlation
% Detailed explanation goes here
% Input parameters in this function:
%     IRP    Initial Reservoir Pressure (Psig)
%     RP     Reservoir Pressure (Psig)
%     OilR   Oil Rate (STB/day)
%     InsD   Instant Well Depth (ft)
%     WHP    Wellhead Pressure (Psig)
%     PD     Estimated Pressure Drop (Psig)
% Output parameters in this function:
%     PDTrue True Pressure Drop (Psig)

% Basic Input Parameters

IRT = 180; %Initial Reservoir Temperature (F)
WHT = 120; %Wellhead Temperature (F)
BHT = 180; %Bottomhole Temperature (F)
TD = 8200; %Total Depth (ft)
Dia = 5.5; %Inner Diameter (in)
Rough = 0.0006; %Pipe Roughness (in)
Angle = 90; %Pipe Inclination Angle with Horizontal
GasG = 0.62; %Gas Gravity
OilAPI = 38.5; %Oil API
OilG = 141.5/(131.5+OilAPI);%Oil Gravity

% Basic Input Parameters End

SD = TD/12;% Step Distance (ft)
BHP = PD+WHP; %Bottomhole Pressure (Psig)
AVP = (WHP+BHP)/2;%Average Pressure (Psig)
AVT = ((WHT + (BHT-WHT)/TD*InsD)+(WHT + (BHT-WHT)/TD*(InsD+SD)))/2;%Average Temperature (F)
IIGOR = GasG*((RP+14.7)/18.2 + 1.4)*10^(0.0125* OilAPI-0.00091*IRT))^(1/0.83);%Instant Intial GOR (scf/STB)
if GasG*((AVP+14.7)/18.2 + 1.4)*10^(0.0125* OilAPI-0.00091*AVT))^(1/0.83)>IIGOR
    GOR = IIGOR;% Solution GOR (scf/STB)
else
    GOR = GasG*((AVP+14.7)/18.2 + 1.4)*10^(0.0125* OilAPI-0.00091*AVT))^(1/0.83);% Solution GOR (scf/STB)
```

```

    end
    if GOR<IIGOR
        Bo = 0.972+1.47*10^(-4)*(1.25*AVT+GOR*(GasG/OilG)^0.5)^1.175;% Oil
Formation Volume Factor (bbl/STB)
    else
        OilC = 10^(-5)*(-1433+5*IIGOR+17.2*AVT-
1180*GasG+12.61*OilAPI)/(RP+14.7); %Oil Compressibility
        Bo = (0.972+1.47*10^(-
4)*(1.25*AVT+GOR*(GasG/OilG)^0.5)^1.175)*exp(OilC*(RP-AVP));% Oil Formation Volume
Factor (bbl/STB)
    end

%Z factor and Gas Formation Volume Factor Calculation
Ppc = 756.8-131.07*GasG-3.6*GasG^2;%Pseudocritical Pressure
Tpc = 169.2+349.5*GasG-74*GasG^2; %Pseudocritical Temperature
Pr = (AVP+14.7)/Ppc; %Pseudoreduced Pressure
Tr = (AVT+460)/Tpc; %Pseudoreduced Temperature
A = 1.39*(Tr-0.92)^0.5-0.36*Tr-0.101;
B = (0.62-0.23*Tr)*Pr+(0.066/(Tr-0.86)-0.037)*Pr^2+0.32/10^(9*(Tr-1))*Pr^6;
C = 0.132-0.32*log10(Tr);
D = 10^(0.3106-0.49*Tr+0.1824*(Tr^2));
Z = A+(1-A)/exp(B)+C*Pr^D;% Z Factor
Bg = 0.0282793*(AVT+460)*Z/(AVP+14.7);% Gas Formation Volume Factor
(rcf/scf)

GasD = 28.97*GasG*(AVP+14.7)/Z/10.73/(460+AVT);% Gas Density (lb/ft3)
if GasG*((AVP+14.7)/18.2 + 1.4)*10^(0.0125* OilAPI-
0.00091*AVT)^(1/0.83)>IIGOR
    OilC = 10^(-5)*(-1433+5*IIGOR+17.2*AVT-1180*GasG+12.61*OilAPI)/(RP+14.7);
    OilD = (350*OilG+0.0764*GasG*GOR)/5.615/Bo*exp(OilC*(AVP-RP));% Oil
Density (lb/ft3)
else
    OilD = (350*OilG+0.0764*GasG*GOR)/5.615/Bo;% Oil Density (lb/ft3)
end
LiqD = OilD;%Liquid Density (lb/ft3)

GasFR = (IIGOR-GOR)* OilR * Bg/86400;% Gas Flowrate (ft3/s)
LiqFR = OilR*Bo*5.615/86400;% Liquid Flowrate (ft3/s)
Area = pi*(Dia/2*0.0833333)^2;% Pipe Sectional Area (ft2)
SfGasFR = GasFR/Area;% Superficial Gas Flowrate (ft/s)
SfLiqFR = LiqFR/Area;% Superficial Liquid Flowrate (ft/s)
SfMixFR = SfGasFR + SfLiqFR;% Superficial Mix Flowrate (ft/s)
GasWFR = GasD * SfGasFR;% Gas Weight Flux Rate (lb/ (ft2.s))
LiqWFR = LiqD * SfLiqFR;% Liquid Weight Flux Rate (lb/ (ft2.s))
MixWFR = GasWFR + LiqWFR;% Mix Weight Flux Rate (lb/ (ft2.s))

```

```

NoSlipHUp = LiqFR/(LiqFR + GasFR);% No-slip Holdup
Nfr = SfMixFR^2/32.174/(Dia*0.0833333);% Froude Number

%Gas Viscosity
Mg = 28.967 * GasG;% Mole weight
K1 = (0.00094+2*10^(-6)*Mg)*(AVT+460)^1.5/(209+19*Mg+(AVT+460));
X = 3.5+986/(460+AVT)+0.01*Mg;
Y = 2.4-0.2*X;
GasVisc = K1*exp(X*(GasD/62.4)^Y); %Gas Viscosity (cp)

DeadOilVisc = 10^(AVT^-1.163*exp(6.9824-0.04658*OilAPI))-1;% Dead Oil
Viscosity (cp)
A1 = 10.715*(GOR+100)^-0.515;
B1 = 5.44*(GOR+150)^-0.338;
if GasG*((AVP+14.7)/18.2 + 1.4)*10^(0.0125* OilAPI-
0.00091*AVT))^(1/0.83)>IIGOR
    C1 = 2.6*AVP^1.187*exp(-11.513+(-8.98*10^-5*AVP));
    OilVisc = A1* DeadOilVisc^B1*(AVP/RP)^C1; % Bubblepoint Oil Viscosity
(cp)
else
    OilVisc = A1* DeadOilVisc^B1; % Bubblepoint Oil Viscosity (cp)
end
LiqVisc = OilVisc;

OilIntT = (1.17013-1.694*10^(-3)*AVT)*(38.085-0.259*OilAPI);% Oil
Interfacial Tension (dynes/cm)
LiqIntT = OilIntT;% Liquid Interfacial Tension (dynes/cm)

MixVisc = 6.72*10^(-4)*(LiqVisc*NoSlipHUp + GasVisc*(1-NoSlipHUp));% Mix
Viscosity (lb/ft/s)
Nre = MixWFR*Dia*0.0833333/MixVisc;% No Slip Reynold Number
Nlv = 1.938*SfLiqFR*(LiqD/LiqIntT)^0.25;% Liquid Velocity Number

%Determine the flow pattern
L1 = 316*NoSlipHUp^0.302;
L2 = 0.0009252*NoSlipHUp^-2.4684;
L3 = 0.1*NoSlipHUp^-1.4516;
L4 = 0.5*NoSlipHUp^-6.738;

if (NoSlipHUp<0.01 && Nfr<L1) || (NoSlipHUp>=0.01 && Nfr<L2)
    Flow = 'Segregated';
elseif (NoSlipHUp>=0.01 && NoSlipHUp<0.4 && Nfr>L3 && Nfr<=L1) ||
(NoSlipHUp>=0.4 && Nfr>L3 && Nfr<=L4)
    Flow = 'Intermittent';
elseif (NoSlipHUp<0.4 && Nfr>=L4) || (NoSlipHUp>=0.4 && Nfr>L4)
    Flow = 'Distributed';

```

```

elseif (Nfr>L2 && Nfr<L3)
    Flow = 'Transition';
else
    Flow = ' ';
end

%Liquid Holdup for Horizontal Flow
SegHup0 = 0.98*NoSlipHUp^0.4846/Nfr^0.0868; % Segregated
InterHup0 = 0.845*NoSlipHUp^0.5351/Nfr^0.0173; % Intermittent
DisHup0 = 1.065*NoSlipHUp^0.5824/Nfr^0.0609; % Distributed

% Selected Liquid Holdup
if strcmp(Flow,'Segregated')
    Sel_Hup0 = SegHup0;
elseif strcmp(Flow,'Intermittent')
    Sel_Hup0 = InterHup0;
elseif strcmp(Flow,'Distributed')
    Sel_Hup0 = DisHup0;
else
    Sel_Hup0 = 1;
end

% Final Selected Liquid Holdup
if Sel_Hup0 > NoSlipHUp
    FSel_Hup0 = Sel_Hup0;
else
    FSel_Hup0 = NoSlipHUp;
end

% Correction Factor Coefficient
SegCF = (1-NoSlipHUp)*log(0.011*NoSlipHUp^(-3.768)*Nlv^3.539*Nfr^(-1.614)); % Segregated Flow
InterCF = (1-NoSlipHUp)*log(2.96*NoSlipHUp^(0.305)*Nlv^(-0.4473)*Nfr^(0.0978)); % Intermittent Flow
DisCF = 0; % Distributed Flow

% Selected Correction Factor Coefficient
if strcmp(Flow,'Segregated')
    Sel_CF = SegCF;
elseif strcmp(Flow,'Intermittent')
    Sel_CF = InterCF;
else
    Sel_CF = DisCF;
end

% Final Selected Correction Factor Coefficient
if Sel_CF <= 0
    FSel_CF = 0;

```

```

    else
        FSel_CF = Sel_CF;
    end

    Rad_Angle = Angle*pi/180; % Pipe Inclination Angle with Horizontal
    B_Angle = 1+FSel_CF*(sin(1.8*Rad_Angle)-(1/3)*sin(1.8*Rad_Angle)^3); %
Correction Factor

%Liquid Holdup for Transition Flow
AA = (L3-Nfr)/(L3-L2);
BB = 1-AA;
SegB_Angle = 1+SegCF*(sin(1.8*Rad_Angle)-(1/3)*sin(1.8*Rad_Angle)^3); %
Correction Factor For Segregated Flow
InterB_Angle = 1+InterCF*(sin(1.8*Rad_Angle)-(1/3)*sin(1.8*Rad_Angle)^3); %
Correction Factor For Intermittent Flow
if SegB_Angle<=1
    SegHup1 = SegHup0;
else
    SegHup1 = SegHup0 * SegB_Angle;
end
if InterB_Angle<=1
    InterHup1 = InterHup0;
else
    InterHup1 = InterHup0 * InterB_Angle;
end
TransHup1 = AA* SegHup1 + BB* InterHup1;
% Selected Liquid Holdup for Transition Flow
if TransHup1<=NoSlipHUp
    Sel_TransHup1 = NoSlipHUp;
else
    Sel_TransHup1 = TransHup1;
end

% Final Liquid Holdup For Next Calculation
if strcmp(Flow,'Transition')
    Final_LiqHup = Sel_TransHup1;
elseif B_Angle<=1
    Final_LiqHup = FSel_Hup0;
else
    Final_LiqHup = FSel_Hup0 * B_Angle;
end
TwoPhaseD = Final_LiqHup * LiqD + (1- Final_LiqHup)*GasD; % two-phase
density
PressDropG = TwoPhaseD * sin(Rad_Angle)/144; % hydrostatic pressure gradient
% Pressure drop due to friction loss
% Ratio of two-phase to no-slip friction factor calculation

```

```

Y = NoSlipHUp/Final_LiqHup^2;
In_Y = log(Y);
S = In_Y/(-0.0523+3.182*In_Y-0.8725*In_Y^2+0.01853*In_Y^4);
if Y == 0
    S_Final = 0;
elseif Y>1 && Y<1.2
    S_Final = log(2.2*Y-1.2);
else
    S_Final = S;
end

FrictionFR = exp(S_Final); % Ratio of two-phase to no-slip friction factor

% No-slip friction factor calculation/ Fanning friction factor calculation
Epsilon_D = Rough/Dia;
FF1 = 64/Nre;
FF2 = 1/(-2*log10(Epsilon_D/3.7+2.51/(Nre*sqrt(FF1))))^2;
FF3 = 1/(-2*log10(Epsilon_D/3.7+2.51/(Nre*sqrt(FF2))))^2;
FF4 = 1/(-2*log10(Epsilon_D/3.7+2.51/(Nre*sqrt(FF3))))^2;
FF5 = 1/(-2*log10(Epsilon_D/3.7+2.51/(Nre*sqrt(FF4))))^2;
FF6 = 1/(-2*log10(Epsilon_D/3.7+2.51/(Nre*sqrt(FF5))))^2;
FF7 = 1/(-2*log10(Epsilon_D/3.7+2.51/(Nre*sqrt(FF6))))^2;
FF8 = 1/(-2*log10(Epsilon_D/3.7+2.51/(Nre*sqrt(FF7))))^2;
FF9 = 1/(-2*log10(Epsilon_D/3.7+2.51/(Nre*sqrt(FF8))))^2;
FF10 = 1/(-2*log10(Epsilon_D/3.7+2.51/(Nre*sqrt(FF9))))^2;
FF11 = 1/(-2*log10(Epsilon_D/3.7+2.51/(Nre*sqrt(FF10))))^2;
FF12 = 1/(-2*log10(Epsilon_D/3.7+2.51/(Nre*sqrt(FF11))))^2;
FF13 = 1/(-2*log10(Epsilon_D/3.7+2.51/(Nre*sqrt(FF12))))^2;
FF14 = 1/(-2*log10(Epsilon_D/3.7+2.51/(Nre*sqrt(FF13))))^2;
FF15 = 1/(-2*log10(Epsilon_D/3.7+2.51/(Nre*sqrt(FF14))))^2;
if Nre<=2100
    FannFriF = FF1 /4; % Fanning friction factor
else
    FannFriF = FF15 /4;
end

TwoPhaseFriF = FrictionFR * FannFriF; % Two-phase friction factor
PressDropF = 2*TwoPhaseFriF*SfMixFR*MixWFR/144/32.174/(Dia*0.0833333); %
pressure gradient due to the friction pressure loss
PressDropT = PressDropG + PressDropF; % Total pressure gradient
PDTrue = SD*PressDropT; % True pressure drop in the length increment
end

```

Appendix B: MATLAB code for natural oil rate calculation

```

function [NOR] = NaturalOilFlow(RP,MaxOilR)
% Summary of this function goes here
% To calculate natural oil flowrate by using IPR and TPR curves
% Detailed explanation goes here
% Input parameters in this function:
% RP Reservoir Pressure (Psig)
% MaxOilR Max Oil Rate (STB/day)
% Output parameters in this function:
% NOR Natural Oil Rate (STB/day)

TD = 8200; %Total Depth (ft)
i= 0;
Oilrate = zeros(1,20);
TPR = zeros(1,20);
IPR = zeros(1,20);
Dif = zeros(1,20);
k =1;
while i< 20
    OilR = 10 + MaxOilR/20*i; % Oil rate
    Oilrate(k) = OilR;
    InsD = 0;% Instant Well Depth (ft)
    WHP = 650; % Wellhead Pressure (Psig)
    L = WHP;
    j = 1;
    % Construct TPR curve
    while InsD < TD
        PressureDropF = @(PD) (PressureDroptest(RP,OilR,InsD,WHP,PD)-PD)^2;
        lb = 0;
        ub = RP;
        x0 = RP/2;
        A = [];
        b = [];
        Aeq = [];
        beq = [];
        nonlcon = [];
        opt = optimoptions('fmincon','Display','off','Algorithm','sqp');
        PDTtrue = fmincon(PressureDropF,x0,A,b,Aeq,beq,lb,ub,nonlcon,opt);
        InsD = j*TD/12;
        L = L+PDTtrue;
        WHP = L;
        j=j+1;
    end
    TPR(k) = L;
end

```

```

IPR(k) = (-0.2+sqrt(0.2^2-4*0.8*(OilR/MaxOilR-1)))/(2*0.8)*RP; % Construct IPR
curve

Dif(k) = IPR(k)-TPR(k); % Pressure difference between IPR and TPR curves
if k>=2
    if Dif(k-1)>0 && Dif(k)<0
        x1 = [Oilrate(k-1),Oilrate(k)];
        y1 = [TPR(k-1),TPR(k)];
        p = polyfit(x1,y1,1);
        func = @(x)((p(1)*x+p(2))-((-0.2+sqrt(0.2^2-4*0.8*(x/MaxOilR-
1)))/(2*0.8)*RP))^2;
        lb = Oilrate(k-1);
        ub = Oilrate(k);
        x0 = Oilrate(k-1);
        A = [];
        b = [];
        Aeq = [];
        beq = [];
        nonlcon = [];
        opt1 = optimoptions('fmincon','Display','off','Algorithm','sqp');
        NOR = fmincon(func,x0,A,b,Aeq,beq,lb,ub,nonlcon,opt1); % Natural Oil
Rate Calculation
    return

end
end
k = k+1;
i = i+1;
end
NOR = 0;

```

Appendix C: MATLAB code for natural gas rate calculation

```
function [NGR] = NaturalGasFlow(RP)
% Summary of this function goes here
% To calculate natural gas flowrate by using IPR and TPR curves
% Detailed explanation goes here
% Input parameters in this function:
% RP      Reservoir Pressure (Psig)
% Output parameters in this function:
% NGR     Natural Gas Rate (MMscf/day)

c = 0.5;% IPR parameter (backpressure equation)
n = 0.7;% IPR parameter (backpressure equation)

WHP = 650; %Wellhead Pressure (Psig)

func1= @(BHPgas) (PressureGasFlow(BHPgas) - (c*(RP^2-BHPgas^2)^n /10^3))^2;
lb = WHP;
ub = RP;
x0 = (WHP+RP)/2;
A = [];
b = [];
Aeq = [];
beq = [];
nonlcon = [];
opt1 = optimoptions('fmincon','Display','off','Algorithm','sqp');
BHPgas = fmincon(func1,x0,A,b,Aeq,beq,lb,ub,nonlcon,opt1);
NGR = c*(RP^2-BHPgas^2)^n /10^3; % Natural Gas Rate Calculation
end
```

Appendix D: MATLAB code for PVT properties calculation

```

function [GOR,Bo,Bg] = PVTproperties(RP)
% Summary of this function goes here
% To calculate PVT properties
% Detailed explanation goes here
% Input parameters in this function:
% RP      Reservoir Pressure (Psig)
% Output parameters in this function:
% GOR     Solution Gas Oil Ratio (scf/STB)
% Bo      Oil Formation Volume Factor (bbl/STB)
% Bg      Gas Formation Volume Factor (bbl/scf)

GasG = 0.62; %Gas Gravity
OilAPI = 38.5; %Oil API
IRT = 180; %Initial Reservoir Temperature (F)

OilG = 141.5/(131.5+OilAPI);%Oil Gravity
Ppc = 756.8-131.07*GasG-3.6*GasG^2;%Pseudocritical Pressure
Tpc = 169.2+349.5*GasG-74*GasG^2; %Pseudocritical Temperature
Tr = (IRT+460)/Tpc; %Pseudoreduced Temperature

GOR = GasG*((RP+14.7)/18.2 + 1.4)*10^(0.0125* OilAPI-0.00091*IRT))^(1/0.83);%
Solution GOR (scf/STB)
Bo = 0.972+1.47*10^(-4)*(1.25*IRT+GOR*(GasG/OilG)^0.5)^1.175;% Oil Formation Volume
Factor (bbl/STB)
Pr = (RP+14.7)/Ppc; %Pseudoreduced Pressure
A = 1.39*(Tr-0.92)^0.5-0.36*Tr-0.101;
B =(0.62-0.23*Tr)*Pr+(0.066/(Tr-0.86)-0.037)*Pr^2+0.32/10^(9*(Tr-1))*Pr^6;
C = 0.132-0.32*log10(Tr);
D = 10^(0.3106-0.49*Tr+0.1824*(Tr^2));
Z = A+(1-A)/exp(B)+C*Pr^D;% Z Factor
Bg = 0.00503676*(IRT+460)*Z/(RP+14.7);% Gas Formation Volume Factor (bbl/scf)
end

```

Appendix E: MATLAB code for the material balance equation

```
function [output] = MBE(N,m,SCNp,SINg,TGOR,Boi,Bgi,GORi,RP)
% Summary of this function goes here
% To construct a function about Material Balance Equation
% Detailed explanation goes here
% Input parameters in this function:
% N Initial oil in place (STB)
% m Initial gas cap-to-oil volume ratio
% SCNp Culmulative Oil Production (STB)
% SINg Culmulative Gas Injection (MMscf)
% Boi Initial Oil Formation Volume Factor (bbl/STB)
% Bgi Gas Formation Volume Factor (bbl/scf)
% GORi Solution Gas Oil Ratio (scf/STB)
% RP Reservoir Pressure (Psig)

[GOR,Bo,Bg] = PVTproperties(RP); % calculate the Bo, Bg, and solution GOR at each
reservoir pressure
output = ((SCNp*(Bo +(TGOR-GOR)*Bg)) - (N*Boi*((Bo-Boi)+(GORi-GOR)*Bg)/Boi) +
(N*m*Boi/Bgi + SINg*10^6)*Bg - N*m*Boi))^2;

end
```

Appendix F: MATLAB code for oil and gas production profiles generation

```

function [Y,Newpressure,Np,Ngp] = UnderGWithdraw(N,m)
% Summary of this function goes here
% To calculate the reservoir pressure decline curve and oil and gas production
profiles
% Detailed explanation goes here
% Input parameters in this function:
% N           Initial oil in place (STB)
% m           Initial gas cap-to-oil volume ratio
% Output parameters in this function:
% Y           Years
% Newpressure Reservoir Pressure (Psig)
% Np          Oil Production (STB/Y)
% Ngp         Gas Production (MMscf/Y)

% Basic Input Parameters

Numberofwells = 20; % Number of wells
MaxOilCap = 18000*365*20; % Maximum Oil Capacity (STB/Y)
Y2MaxOilR = 5.5; % Years to reach the Maxmium Oil Rate
MaxGasCap = 21.1*365*20;% Maximum Gas Capacity (MMscf/Y)
Pgy = 1000;% The year to start to produce free gas
Y2MaxGasR = 4; % Years to reach the Maxmum Gas Rate
IRP = 4263; % Initial Reservoir Pressure (Psig)
MaxOilR = 50000; % Maximum Oil Rate (STB/Y)

%Basic Input Parameters End

[GORi,Boi,Bgi] = PVTproperties(IRP); % Initial Bo, Bg, and Solution GOR calculation

Newpressure = zeros(200,1); Newpressure(1)= IRP;

Y = zeros(200,1); Y(1) = 0; % Year
Nr = zeros(200,1); Nr(1) = N;% Remaining Oil Volume
Np = zeros(200,1);Np(1) = 0; % Real Oil Production
Ngp = zeros(200,1);Ngp(1) = 0; % Real Gas Production
CNp = zeros(200,1);CNp(1) = 0;% Real Culmulative Oil Production
Nsdp = zeros(200,1);Nsdp(1)= 0;% Real Solution Gas Production
CNSdp = zeros(200,1);CNSdp(1)=0;% Real Culmulative Solution Gas Production
ING = zeros(200,1);ING(1) = 0;% Culmulative Gas injection
Nfgp = zeros(200,1);Nfgp(1) = 0;% Real Free Gas Production
GasCapNgp = zeros(200,1);% Gas Production due to the capacity influence
CNTgp = zeros(200,1); % Real Culmulative total Gas Production
Ngr = zeros(200,1); Ngr(1)=N*m*Boi/Bgi/10^6;% Remaining gas volume

Py =1;
RPj = IRP;

```

```

MaxOilRj = MaxOilR;
gy =1;

while Nr(Py) >0
    Y(Py+1) = Py;
    if Py >2 && Np(Py) == 0
        OilR_Year = 0;
    else
        OilR_Day = NaturalOilFlow(RPj,MaxOilRj);
        OilR_Year = OilR_Day*365*Numberofwells;% Oil production in one year (STB/Year)
    end

    if Py < Y2MaxOilR
        OilCap = MaxOilCap/Y2MaxOilR * Py;
    else
        OilCap = MaxOilCap;
    end

SmaP = [OilCap, OilR_Year, Nr(Py)];
Np(Py+1) = min(SmaP);
CNp(Py+1) = CNp(Py)+min(SmaP);
Nr(Py+1) = Nr(1)-CNp(Py+1);
Nsgp(Py+1) = Np(Py+1)* PVTproperties(RPj)/10^6;
CNsgp(Py+1) = CNsgp(Py) + Nsgp(Py+1);
INg(Py+1) = CNsgp(Py+1);

if Py < Pgy
    Ngr(Py+1) = Ngr(1) + INg(Py+1);
    TGOR = CNsgp(Py+1)/CNp(Py+1)*10^6;
    SCNp = CNp(Py+1);
    SING = INg(Py+1);
    AAA = @(RP) MBE(N,m,SCNp,SING,TGOR,Boi,Bgi,GORi,RP);
    opt = optimoptions(@fminunc,'Display','off','Algorithm','quasi-newton');
    Newpressure(Py+1) = fminunc(AAA,Newpressure(Py),opt);
else
    Nfgp(Py+1) = NaturalGasFlow(RPj)*365*Numberofwells;
    if gy < Y2MaxGasR
        if (Nsgp(Py+1)+ Nfgp(Py+1)) > MaxGasCap
            INg(Py+1) = MaxGasCap*(1-gy/Y2MaxGasR) + INg(Py);
            CNsgp(Py+1) = MaxGasCap + CNsgp(Py);
            GasCapNgp(Py+1) = MaxGasCap*gy/Y2MaxGasR;
            Fgi = INg(Py+1);
        else
            INg(Py+1) = (Nsgp(Py+1)+ Nfgp(Py+1))*(1-gy/Y2MaxGasR) + INg(Py);
            CNsgp(Py+1) = (Nsgp(Py+1)+ Nfgp(Py+1))+ CNsgp(Py);
            GasCapNgp(Py+1) = (Nsgp(Py+1)+ Nfgp(Py+1))*gy/Y2MaxGasR;
    end
end

```

```

        Fgi = INg(Py+1);
    end
else
    if (Nsgp(Py+1)+ Nfgp(Py+1)) > MaxGasCap
        INg(Py+1) = Fgi;
        CNsgp(Py+1) = MaxGasCap + CNsgp(Py);
        GasCapNgp(Py+1) = MaxGasCap;
    else
        INg(Py+1) = Fgi;
        CNsgp(Py+1) = (Nsgp(Py+1)+ Nfgp(Py+1))+ CNsgp(Py);
        GasCapNgp(Py+1) = (Nsgp(Py+1)+ Nfgp(Py+1));
    end
end
gy = gy +1;
SmaGP = [GasCapNgp(Py+1),Ngr(Py)];
Ngp(Py+1) = min(SmaGP);
CNTgp(Py+1) = CNTgp(Py)+ min(SmaGP);
Ngr(Py+1) = Ngr(1)+ INg(Py+1)- CNTgp(Py+1);
TGOR = CNsgp(Py+1)/CNp(Py+1)*10^6;
SCNp = CNp(Py+1);
SING = INg(Py+1);
AAA = @(RP) MBE(N,m,SCNp,SING,TGOR,Boi,Bgi,GORi,RP);
opt = optimoptions(@fminunc,'Display','off','Algorithm','quasi-newton');
Newpressure(Py+1) = fminunc(AAA,Newpressure(Py),opt);
end
MaxOilRj = Newpressure(Py+1)/IRP*MaxOilR;
RPj = Newpressure(Py+1);
if Np(Py+1) == 0 && Ngp(Py+1)== 0
    return
end
if Py >198
    return
end
Py = Py+1;
end
end

```

Appendix G: MATLAB code for the PERT distribution

```

function [OilV, GasV, OilVmean, OilVstd, GasVmean, GasVstd] = PERTdistribution()
% Summary of this function goes here
% To generate the PERT distribution for oil in place and gas cap-to-oil volume
ratio
% Detailed explanation goes here
% Output parameters in this function:
%     OilV      Oil in place (MMSTB)
%     GasV      Gas cap-to-oil volume ratio
%     OilVmean    Mean of oil in place distribution
%     OilVstd     Standard deviation of oil in place distribution
%     GasVmean    Mean of gas cap-to-oil volume ratio distribution
%     GasVstd     Standard deviation of gas cap-to-oil volume ratio distribution

% Basic Input Parameters
OilVmin = 2000; % minimum value of oil in place (MMSTB)
OilVmode = 4000; % mode of oil in place (MMSTB)
OilVmax = 15000; % maximum value of oil in place (MMSTB)

GasVmin = 0.2; % minimum value of gas cap-to-oil volume ratio
GasVmode = 0.4; % mode of gas cap-to-oil volume ratio
GasVmax = 1.2; % maximum value of gas cap-to-oil volume ratio
% Basic Input Parameters End

N_samples = 1000; % number of samples

OilVmean = (OilVmin+4*OilVmode+OilVmax)/6;
OilVstd = (OilVmax-OilVmin)/6;
Oilw1 = (OilVmean-OilVmin)*(2*OilVmode-OilVmin-OilVmax)/(OilVmode-
OilVmean)/(OilVmax-OilVmin);
Oilw2 = Oilw1*(OilVmax-OilVmean)/(OilVmean-OilVmin);
OilVdist = makedist('Beta','a',Oilw1,'b',Oilw2);
rng('shuffle');y1 = rand(N_samples,1);
OilVbeta = icdf(OilVdist,y1);
OilV= OilVbeta * (OilVmax-OilVmin) + OilVmin;

GasVmean = (GasVmin+4*GasVmode+GasVmax)/6;
GasVstd = (GasVmax-GasVmin)/6;
Gasw1 = (GasVmean-GasVmin)*(2*GasVmode-GasVmin-GasVmax)/(GasVmode-
GasVmean)/(GasVmax-GasVmin);
Gasw2 = Gasw1*(GasVmax-GasVmean)/(GasVmean-GasVmin);
GasVdist = makedist('Beta','a',Gasw1,'b',Gasw2);
rng('shuffle');y2 = rand(N_samples,1);
GasVbeta = icdf(GasVdist,y2);
GasV= GasVbeta * (GasVmax-GasVmin) + GasVmin;

end

```

Appendix H: MATLAB code for Monte Carlo simulation

```
% Summary of this function goes here
% Monte Carlo simulation application and parallel computing

[OilV, GasV, OilVmean, OilVstd, GasVmean, GasVstd] = PERTdistribution() ;

Np = zeros(200,length(OilV));
Ngp = zeros(200,length(OilV));
Newpressure = zeros(200,length(OilV));
Year = transpose(0:1:199);

parfor i = 1:length(OilV)
    [Y, Newpressure(:,i), Np(:,i), Ngp(:,i)] = UnderGWithdraw(OilV(i)*10^6, GasV(i));
end
```